Mod5 mediates a molecular trade-off between optimal gene expression and antifungal resistance.

Alexander Bruch[1]†, Valentina Lazarova[1]†, Thomas Krüger[2], Sascha Schäuble[3], Abdulrahman A. Kelani[1], Pamela Lehenberger[1], Olaf Kniemeyer[2], Gianni Panagiotou[3,4,5], Matthew G. Blango[1]*

[1] Junior Research Group RNA Biology of Fungal Infections, Leibniz Institute for Natural Product Research and Infection Biology—Hans Knöll Institute (Leibniz-HKI), Jena, Germany.

[2] Department of Molecular and Applied Microbiology, Leibniz Institute for Natural Product Research and Infection Biology—Hans Knöll Institute (Leibniz-HKI), Jena, Germany.

[3] Department of Microbiome Dynamics, Leibniz Institute for Natural Product Research and Infection Biology—Hans Knöll Institute (Leibniz-HKI), Jena, Germany.

[4] Department of Medicine and State Key Laboratory of Pharmaceutical Biotechnology, University of Hong Kong, Hong Kong, China.

[5] Cluster of Excellence Balance of the Microverse, Friedrich-Schiller-University Jena, Jena, Germany.

† Joint Authors are listed in alphabetical order.

*Correspondence: E-mail matthew.blango@leibniz-hki.de; Tel. +49 (0)3641-532 1072.

ABSTRACT

Increasing antifungal drug resistance is a major concern associated with human fungal infections. Genetic mutation and epimutation mechanisms are clear drivers of resistance, yet the epitranscriptome remains relatively untested regarding resistance. Here, deletion of the *Aspergillus fumigatus* tRNA-modifying isopentenyl transferase ortholog, Mod5, led to altered stress response and unexpected resistance against the antifungal drug 5-fluorocytosine (5-FC). Simultaneous profiling of transcriptomes and proteomes revealed comparable general adaptation to 5-FC stress; however, a premature activation of cross-pathway control (CPC) genes in the knockout was further increased after antifungal treatment. By associating codon usage patterns with proteomics abundances, we observed a negative correlation with the number of $tRNA^{Tyr}_{G\Psi A}$-decoded codons in the knockout, indicative of modification-tuneable transcripts. Subsequent overexpression of $tRNA^{Tyr}_{G\Psi A}$ in the Δ*mod5* strain rescued select phenotypes but failed to reverse 5-FC resistance. Investigation of the purported tRNA gene-mediated silencing function of Mod5 uncovered a negative correlation between tRNA proximity and gene induction under normal growth, indicating an active pathway. In conclusion, 5-FC resistance in the absence of Mod5 likely originates from multifaceted transcriptional and translational changes that skew the fungus towards starvation responses over optimal growth, offering a mechanism reliant on RNA modification and tRNA gene-mediated silencing to facilitate transient antifungal resistance.

INTRODUCTION

Severe fungal infections have increased constantly in recent decades and represent a substantial threat to human health, resulting in over a billion infections and roughly 3.75 million deaths per year (GAFFI.org, (1-3)). In 2022, this danger was recognized by the World Health Organization (WHO) as a prioritized list of fungal species, based on infectivity, severity of infection, and propensity for antifungal resistance (4). Among the critical priority group of fungal pathogens is *Aspergillus fumigatus*, a filamentous saprophytic fungus that resides in the environment but is able to reach the lungs of human hosts as airborne asexual spores, termed conidia (5). In healthy individuals, the innate immune system eliminates invading spores, whereas heavily immunocompromised patients are susceptible to outgrowth of the conidia and dangerous invasive infections (6,7). Treatment of these infections relies on a limited set of antimycotics, including the echinocandins, polyenes, and azoles, of which the latter represents the first-line medication used to treat *A. fumigatus* infections (8,9). Other potential drugs like 5-fluorocytosine (5-FC; flucytosine) are normally used in combinatorial antifungal treatments but are not used to treat *A. fumigatus* infections due to swift development of resistance (5,8,10). Additionally, development of antifungal resistance is further amplified by heavy utilization of molecularly similar drugs in agriculture, creating a selective environmental pressure (11,12).

Clearly, a better understanding of the molecular mechanisms underlying resistance and virulence are needed to combat the problem of human fungal infections.

Many studies have investigated genomic-encoded resistance, but much less is known about the role of the more than 170 known RNA chemical modifications, termed the epitranscriptome, in control of resistance and virulence (13,14). RNA modifications are particularly prevalent on transfer RNAs (tRNA), where these range from simple methylations (e.g., 5-methyl cytosine=m^5C) or isomerisations (e.g. pseudouridine=Ψ) to complex chemical groups like N^6-isopentenyl adenosine (i^6A). Modifications fulfil a variety of functions, for example by supporting the integrity of the tRNA tertiary structure or translational fidelity (13,15). The highly-conserved i^6A modification is installed at position 37 of select adenosines in the anticodon stem-loop by isopentenyl transferases (IPTase) to support base stacking, prevent cross-anticodon stem-loop base pairing between U_{33} and A_{37}, and fine-tune codon-anticodon interactions (16-20).

The i^6A modification has been investigated in multiple model systems to assess the physiological consequences in pathogenic organisms. Deletion of the IPTase *miaA* in the bacterium *Shigella flexneri* resulted in the absence of i^6A_{37} and its derivative $ms^2i^6A_{37}$ and strongly decreased the expression of different virulence factors (21). Interestingly, these changes only occurred on the translational but not transcriptional level, indicating a regulatory dependency of pathogenicity on the presence of i^6A/ms^2i^6A-modified tRNAs. In more recent work, the role of MiaA and corresponding tRNA modification in stress adaptation and virulence was shown for extraintestinal pathogenic *Escherichia coli* (ExPEC) (22). Oscillation of the modifier during stress situations clearly indicated an active adaptation of the i^6A/ms^2i^6A tRNA modification pattern in ExPEC that affected the translational capacity of the bacteria and modulated the composition of the proteome. This was even more apparent as soon as the MiaA level was artificially changed by either ablation or overexpression (22), suggesting that MiaA could function as a molecular rheostat for control of stress response.

We hypothesized that similar regulation likely exists in fungal pathogens, and a few studies have indeed reported that the epitranscriptome contributes to fungal virulence and stress resistance. For instance, a study focusing on the kinome of *Cryptococcus neoformans* revealed that specific tRNA modification-relevant kinases, namely *BUD32*, *TRM7,* and *TRM4*, are important for its pathogenicity (23). These findings were underscored by a recent report focusing on Sua5, which in cooperation with Bud32 (and other proteins), is responsible for t^6A_{37} tRNA modification, pointing out its significance for fungal virulence (24). Similarly, several papers recently described how the modulation or ablation of mcm^5/s^2U_{34}, affected the

metabolism, stress adaptivity, and virulence of *Candida albicans*, *Magnaporthe oryzae,* and *A. fumigatus* (25-27). These studies suggest that anticodon stem-loop modifications, specifically at position 34 and 37, have been underestimated for their relevance in host-fungal interactions.

Little is known of the function of i^6A_{37} in pathogenic fungi, with many insights of fungal IPTase-dependent modifications coming from non-pathogenic model systems like *S. cerevisiae* or *S. pombe* (14,16,28). In bakers' yeast, Mod5 can localize to different cellular compartments to install i^6A on cytoplasmic and mitochondrial tRNAs, but it also translocates into the nucleus to perform tRNA gene-mediated silencing (TGM), a secondary transcription regulatory function (29-36). Interestingly, the yeast protein also contains a prion domain that enables it to form amyloid structures (37). The shift from soluble protein to prion form (and back) was found to not only influence the modification function of Mod5 but also represents a molecular switch to adapt to azole drugs, providing a connection between tRNA modification and antifungal drug resistance (37). Despite its many functions, deletion of *MOD5* is well compensated by bakers´ yeast and led to few phenotypes beyond slight sporulation defects and decreased suppressor efficiency of $tRNA^{Tyr}_{UAA}$ (16,19). Similar to *S. cerevisiae*, deletion of the IPTase *TIT1* in *S. pombe* also resulted in few phenotypes, limited to increased sensitivity against rapamycin treatment, reduced translation, and mitochondrial dysfunction when grown on non-fermentable carbon sources (38,39). Interestingly, despite multiple cytoplasmic and mitochondrial tRNAs being modified by Tit1, overexpression of the hypomodified cy-$tRNA^{Tyr}_{G\Psi A}$ reverted the observed phenotypes, indicating that this tRNA was strongly affected by lack of i^6A_{37} in *S. pombe* (38). In summary, proper tRNA modification is a prerequisite for pathogenesis, with surprising implications on antifungal drug resistance.

Here, we present evidence that deletion of *mod5* impacts the transcriptome, translational capacity, and stress response of the opportunistic fungal pathogen *A. fumigatus*. Surprisingly, deletion of this bifunctional tRNA modification enzyme resulted in increased resistance of the fungus against the antimycotic agent 5-fluorocytosine, while also displaying varying susceptibilities against other tested antifungal drugs. The mechanism of 5-FC resistance appeared multifaceted, relying on both the canonical tRNA modification function and the role of Mod5 in tRNA gene-mediated silencing.

MATERIAL AND METHODS

Culture and growth conditions

Aspergillus fumigatus strains used in this study (**Tab. S18**) were cultivated on AMM agar plates according to (40) at 37°C. Spores from respective agar plates were harvested after 5 days utilizing a T-cell scraper, suspended in 10 mL sterile water, and filtered through a 30- µm cell

strainer (MACS, Miltenyi Biotec GmbH; Bergisch Gladbach, Germany) to remove remaining mycelium. Spore concentration was determined using a Roche Innovatis CASY Cell Counter & Analyzer System Modell TT. For liquid cultures, $1x10^8$ or $5x10^7$ *A. fumigatus* spores were cultured in 50 mL AMM for a selected time (24-48 h) at 37°C and 200 rpm. Mycelial balls were harvested using Miracloth (EMD Millipore Corp., USA) and rinsed with ultrapure Milli-Q® water (Merck Millipore, Germany). Positive *A. fumigatus* transformants were selected from AMM agar plates that were supplemented with either pyrithiamine (0.1 µg/mL) or phleomycin (80 µg/mL). *E. coli* cultures were grown in LB media at 37°C and supplemented with 60 µg/mL carbenicillin as necessary.

Droplet Stress Assays

The droplet stress assays were conducted with freshly harvested spores from five-day cultures. Spore suspensions were adjusted to a concentration of $2x10^7$ spores/mL in sterile water corresponding to $1x10^5$ spores in 5 µL. Ten-time dilutions of 10^5- 10^2 spores/5 µL were spotted on square petri dishes containing 50 mL of AMM which were supplemented with 500 ng/mL or 750 ng/mL rapamycin, 0.3 mM 3-Amino-1,2,4 Triazole (3-AT), 0.4 µg/mL 5-fluoroorotic acid (5-FOA), 1 ng/µL, 40 ng/µL or 80 ng/µL fluorocytosine (5-FC), 40 µg/mL hygromycin, 0.1 µg/mL itraconazole, 0.5 µg/mL tebuconazole, 0.25 µg/mL voriconazole and 0.5 µg/mL or 8 µg/mL caspofungin. Assays were incubated at 37°C for 48 and 72 h and documented using a Nikon D6500 AF-S NIKKOR 18-105mm f/3.5-5 ED VR camera.

Minimal inhibitory concentration assays (MICs)

The MICs were determined by suspending wild-type and Δ*mod5* spores in 96-well plates containing RPMI 1640 Medium (Thermo Fisher Scientific), adjusted to a final concentration of 2% glucose (v/v) and grown for 48 h. Each well contained increasing concentrations of the antifungal compound, as well as positive and sterile controls up to a total volume of 200 µL. Spore dilutions of $2x10^7$, of both wild type and knockout were prepared in 2% glucose RPMI, for a final inoculum concentration of $1x10^5$ total spores per well (5 µL). The antifungal agent, 5-FC, was sterilized using 0.22-µm sterile filter (Carl Roth, Germany) and diluted in 1x RPMI 2% glucose (v/v) to attain the desired concentrations. Visual assessment of hyphal growth to elucidate the MIC was performed on a black and white paper background.

Strategies for genetic manipulation of *A. fumigatus*

Generation of *mod5* knockout- or $tRNA^{Tyr}_{G\Psi A}$-overexpression constructs relied on the Gibson cloning method. The deletion approach was conducted according to (40) amplifying a selection gene together with flanking sequences of about 1kb of the *mod5* (*AFUB_093210*) gene employing the primer pair given in **Tab. S19**. $tRNA^{Tyr}_{G\Psi A}$-overexpression construct was

generated by cloning 3 PCR products: $tRNA^{Tyr}_{G\Psi A}$ gene (*AFUB_013600*), a vector backbone (consisting of pyrG flanking regions; phleomycin resistance marker; and tetracycline-inducible promoter), and synthesized *Aspergillus nidulans* Ttef transcriptional terminator. $tRNA^{Tyr}_{G\Psi A}$ gene and Ttef were amplified using primer pairs (oARK0158 & oARK0159) and (oARK0160 & oARK0161), respectively. The vector backbone was amplified from a previously described plasmid pSilent-*pksP* 2 (40) using primer pair oARK0154 and oARK0157.

Insertion of the $tRNA^{Tyr}_{G\Psi A}$-overexpression construct or deletion of *mod5* in *A. fumigatus* CEA17 Δ*akuB*^{KU80} was achieved by protoplast transformation and homologous recombination following the instructions of (41).

RNA Extraction and processing

For RNA extraction from fungal mycelia, $1x10^8$ spores were inoculated in 50 mL AMM and grown for 16 to 24 h (+ 4-8 h with appropriate 3-AT or 5-FC stressors, respectively) at 37°C and 200 rpm. Afterwards, mycelia were harvested using Miracloth (EMD Millipore Corp., USA), rinsed with sterile water and same amounts of mycelium were transferred to 2-mL screw cap tubes for RNA isolation. All centrifugation steps were performed at 4°C and full speed (20,817 x *g*). 800 µL of TRIzol (Thermo Fischer Scientific, Dreieich) were added to each tube, along with glass beads (1/3 of the tube) and the mycelium was mechanically disrupted by 3 rounds of 30 sec, 4.0 m/sec homogenization using the FastPrep-24™ Homogenizer. Subsequently, the samples were incubated for 5 min on ice, followed by additional 5 min at room temperature. After addition of 160 µL of chloroform, the samples were vigorously vortexed for 10 sec and centrifuged for 5 min. The resulting aqueous phase containing the RNA was carefully transferred to a new RNase-free tube without disturbing the interphase. The RNA phase was then purified using the same amount of phenol/chloroform/isoamyl alcohol and centrifuged for 5 min. The purification step was repeated 2-3 times until the interphase remained clear. In the next step, RNA was further purified with 400 µL of chloroform and centrifugation for 5 min. The aqueous phase was again transferred to a new RNase-free 2-mL tube, precipitated by addition of 500 µL isopropanol for 20 min, and RNA was pelleted by 20 min centrifugation. The RNA pellet was washed with 70% ethanol (v/v) and air-dried at 37°C. Finally, RNA was dissolved in 30-50 µL DEPC water at 65°C. The RNA was purified using the RNA Clean and Concentrator™ kit (Zymo Research, USA) following the manufacturer's instructions. Up to 10 µg of total RNA was afterwards treated with 2 U of DNase I endonuclease (Thermo Fisher) for 30-60 min at 37°C in a volume of 20 µL. RNA concentration was then quantified with the Qubit™ RNA BR Assay kit (Thermo Fisher Scientific) on the Qubit Flex Fluorometer (Thermo Fisher Scientific). Quality was assessed either by agarose gel electrophoresis or QUBIT™ Integrity and Quality (IQ) kit (Thermo Fisher).

Quantitative reverse transcription PCR (qRT-PCR)

Prior to qRT-PCR analysis, complementary DNA (cDNA) was synthesized from 200 ng RNA templates using the Maxima H Minus Reverse Transcriptase kit (Thermo Fisher) following the manufacturer instructions. The cDNA concentration was quantified using the Qubit Flex Fluorometer (Thermo Fisher Scientific). qRT-PCR reactions were conducted using the Luna Universal qPCR Master Mix (New England BioLabs) according to manufacturer instructions. Each reaction contained 1 ng cDNA template. Technical triplicates for four to six biological replicates were performed for each experiment. The qRT-PCR program ran on QuantStudio 3 Real Time PCR System (Thermo Fisher), with the temperature profile in accordance with the Luna Universal qPCR Master Mix instructions. The threshold value (Ct) was determined by default settings. Relative expression was calculated using the $2^{-\Delta\Delta CT}$ method (42) and was normalized to the expression values of *cox5* housekeeping gene (40).

mRNA Sequencing and analysis

For mRNA sequencing, CEA17 Δ*akuB*^{KU80} and Δ*mod5* fungal samples ($5x10^7$ spores) were cultured either for 24 h or for 16 h in AMM followed by an 8-h treatment with 80 ng/µL of 5-FC. RNA isolation and purification were carried out as explained above. The extracted RNA samples were subsequently submitted to Novogene (England) for quality control, library preparation, and mRNA sequencing. Sequencing was performed on the Illumina NovaSeq 6000 Sequencing System, using 150-bp paired-end sequencing. The raw data output, provided in FASTQ format by Novogene, was checked for quality, aligned to the A1163 fungal genome (Ensembl), and assessed for differential gene expression in accordance to (40). Briefly, pre-processing of raw reads, quality control and gene abundance estimation used GEO2RNaseq pipeline (v0.100.3, (43)) in R (version 3.6.3). Quality analysis was performed with FastQC (v0.11.5) before and after trimming. Read-quality trimming was done with Trimmomatic (v0.36) and reads were rRNA-filtered using SortMeRNA (v2.1) with a single rRNA database combining all rRNA databases shipped with SortMeRNA. Reference annotation was created by extracting and combining exon features from annotation files. Reads were mapped against reference genome of *A. fumigatus* (A1163, assembly GCA_000150145.1) using HiSat2 (v2.1.0, paired-end mode). Gene abundance estimation was done with featureCounts (v2.0.1) in paired-end mode with default parameters. MultiQC version 1.7 was used to summarize and assess quality of output from FastQC, Trimmomatic, HiSat, featureCounts and SAMtools. The count matrix with gene abundance data without and with median-of-ratios normalization (MRN, (44)) were extracted. Differential gene expression was analyzed with GEO2RNaseq. Pairwise tests were performed using four statistical tools (DESeq v1.38.0, DESeq2 v1.26.0, limma voom v3.42.2 and edgeR v3.28.1) to report *p*-values and multiple

testing corrected *p*-values with false-discovery rate method q = FDR(p) used for each tool. Mean MRN values were computed per test per group including corresponding log2 of fold-changes. Gene expression differences were considered significant only if reported significant by all four tools ($q \leq 0.05$) and $|\log2(\text{fold-change [MRN based]})| \geq 1$.

Northern Blotting

Northern blots were performed to visualize tRNA expression patterns. The RNA probe was labelled using a DIG oligonucleotide tailing kit (Roche, Germany), as per the manufacturer's instructions. 5-10 µg of DNase-treated RNA samples were denatured for 3 min at 70°C and separated on a 15% (w/v) TBE-urea gel (Novex®) with a low range ssRNA ladder (New England Biolabs, USA). The gel was stained with 1x SYBR gold dye (Thermo Fisher Scientific GmbH, Dreieich) and imaged with AlphaImager™ (Biozym Scientific GmbH) imaging system. Subsequently, the RNA was transferred to a Roti®-Nylon plus membrane (pore size of 0.45 µM) with sufficient volumes of transfer buffer (10x SSC) for 4 h or overnight. Following capillary transfer, RNA-to-membrane-crosslinking was performed by UV-irradiation (2 min, E=1200 $\mu J/cm^2$) and the membrane was subjected to pre-hybridization for 1 h at 37-55°C (depending on probe) adding 20 mL of hybridization buffer (1 g dextran sulfate, 13.8 mL sterile water, 5 mL 20x SSC buffer, 10% SDS (w/v), 1 mL of 10x Western blocking reagent (Roche GmbH; Mannheim, Germany)). Hybridization was performed overnight after adding 25 pmol of the DIG-11-dUTP labelled probe. The membrane was washed at RT employing wash buffer I (1x SSC, 0.1% SDS) and wash buffer II (0.5xSSC, 0.1% SDS) for 5 min each. Afterwards, it was rinsed with 50 mL maleic acid buffer (0.15M NaCl, pH 7.5- adjusted with NaOH pellets) for 5 min prior incubation with blocking solution (30 min, 5rpm; 18 mL maleic acid buffer, 2 mL 10X Western Blocking reagent). The incubation was continued for another 30 min after addition of 0.5 µL of Anti-Digoxigenin-AP, Fab fragments (Roche, Mannheim, Germany). Unbound antibodies were eliminated by washing with 50 mL maleic acid buffer + 150 µL Tween 20 (Sigma Aldrich) for 15 min. Subsequently, the membrane was equilibrated by several washes with detection buffer (0.1 M Tris, 0.1 M NaCl, pH 9 – adjusted with HCl) and then incubated with CDP-Star substrate (Roche, Germany) for 5 min in darkness. The chemiluminescent signal was detected using the Chemiluminescence Imaging - Fusion FX SPECTRA (Vilber Lourmat, Collégien France). Potential reuse of the blots was executed by stripping with 0.5% SDS (w/v) for 1 h at 60°C, and re-hybridizing with a control probe.

Southern Blot

Validation of target gene deletion or gene insertion in *A. fumigatus* were conducted by analytic DNA digestions and subsequent Southern Blot according to (40,45).

Protein Extraction

Protein extraction for LC-MS/MS proteome analysis utilized the same hyphal samples as the mRNA sequencing. Equivalent amounts (~ 50 mg) of mycelia were disrupted with mortar and pestle in liquid nitrogen, transferred into 1.5 mL screw cap tubes and mixed thoroughly with 300 µL of freshly prepared lysis buffer (1% SDS (w/v), 150 mM NaCl, 100 mM TEAB (triethyl ammonium bicarbonate), 1 tablet Complete Ultra Protease Inhibitor Cocktail/PhosSTOP (Roche), ultrapure water). After addition of Benzonase nuclease (100 U) the samples were subjected to 30-minute sonication (Bandelin Sonorex Super RK 510 H) at 37°C. To remove insolubilized debris, the samples were centrifuged (4°C, 15 min, 20000 g) and the supernatant was further processed. Protein concentration was assessed using Merck Millipore Direct Detect System. 100 µg of protein was mixed with 100 mM TEAB, 2 µL reduction buffer (500 mM TCEP (tris(2-carboxyethyl) phosphine), 100 mM TEAB), and 2 µL freshly prepared alkylation buffer (625 mM 2-chloroacetamide dissolved in 100 mM TEAB). Afterwards, the samples were incubated at 70°C and 500 rpm in the dark for 30 min. Proteins were precipitated by MeOH/chloroform/water according to the protocol of Wessel and Flügge (46). Subsequently the pellet was dried in Concentrator plus (Eppendorf, Hamburg, Germany) and the protein precipitate was resolubilized in 100 µL of 100 mM TEAB in 5% (v/v) 2,2,2-trifluoroethanol and sonicated for 15 min. Next, Trypsin/LysC protease mix (2 µg/ µL, Promega) was added (1:25 protease: protein ratio) and incubated for 20 h at 37°C. Samples were afterwards dried in Concentrator plus (Eppendorf, Hamburg, Germany) and resolubilized in 30 µL 0.05% TFA, 2% acetonitrile in water. Following this, ultrasonic bath treatment (15 min) and subsequent vortexing homogenized the samples. Filtration was then performed through 10 kDa MWCO spin filter (VWR), at 14 000 × *g* for 15 min at 8°C and the samples were transferred into high-performance liquid chromatography vials for further analysis.

LC-MS/MS

Liquid Chromatography-Tandem Mass Spectrometry analysis was performed according to (40), with slight adjustments mentioned in text below. Each biological sample was measured in three technical replicates. Analysis was conducted with Ultimate 3000 nano RSLC system coupled to Orbitrap Exploris 480 mass spectrometer (both Thermo Fisher Scientific, Waltham, MA, USA) with FAIMS. Peptide trapping took 5 min on an Acclaim Pep Map 100 column (2 cm x 75 µm, 3 µm) at 5 µL/min. This was followed by separation on an analytical Acclaim Pep Map RSLC nano column (50 cm x 75 µm, 2µm). Mobile phase gradient elution employed eluent A (0.1% (v/v) formic acid in water) mixed with eluent B (0.1% (v/v) formic acid in 90/10 acetonitrile/water). The following gradient was utilized: 0 min at 4 % B, 20 min at 6 % B, 45 min at 10 % B, 75 min at 16 % B, 105 min at 25 % B, 135 min at 45 %, 150 min at 65 %, 160-165 min at 96% B, 165.1-180 min at 4% B. Positively charged ions were generated at spray

voltage of 2.2 kV with stainless steel emitter attached to Nanospray Flex Ion Source (Thermo Fisher). Quadrupole/orbitrap instrument operated in Full MS / data-dependent MS2 mode. Precursor ions were monitored at m/z 300-1200 at a resolution of 120,000 FWHM (full width at half maximum) using a maximum injection time (ITmax) of 50 ms and 300% normalized AGC (automatic gain control) target. Precursor ions with a charge state of z=2-5 were filtered at an isolation width of m/z 4.0 amu for further fragmentation at 28% HCD collision energy. MS2 ions were scanned at 15,000 FWHM (ITmax=40 ms, AGC= 200%) with three different compensation voltages being applied (-48 V, -63 V, -78 V).

Protein database search

Tandem mass spectra were searched against the UniProt pan proteome database (2023/07/14) of *Aspergillus fumigatus* (https://ftp.uniprot.org/pub/databases/uniprot/current_release/knowledgebase/pan_proteomes/UP000002530.fasta.gz) using Proteome Discoverer (PD) 3.0 (Thermo) and the database search algorithms (threshold search engine scores in parenthesis) Chimerys (>2), Mascot 2.8 (>30), Comet (>3), MS Amanda 2.0 (>300), Sequest HT (>3) with and without INFERYS Rescoring . Two missed cleavages were allowed for the tryptic digestion. The precursor mass tolerance was set to 10 ppm and the fragment mass tolerance was set to 0.02 Da. Modifications were defined as dynamic Met oxidation, phosphorylation of Ser, Thr, and Tyr, protein N-term acetylation with and without Met-loss as well as static Cys carbamidomethylation. A strict false discovery rate (FDR) < 1% (peptide and protein level) was required for positive protein hits. The Percolator node of PD3.0 and a reverse decoy database was used for q-value validation of spectral matches. Only rank 1 proteins and peptides of the top scored proteins were counted. Label-free protein quantification was based on the Minora algorithm of PD3.0 using the precursor abundance based on intensity and a signal-to-noise ratio >5. Normalization was performed by using the total peptide amount method. Imputation of missing quan values was applied by using abundance values of 75% of the lowest abundance identified per sample. Differential protein abundance was defined as a fold change of >2, pvalue/ABS(log4ratio) <0.05 (pvalue/log4ratio) and at least identified in 2 of 3 replicates of the sample group with the highest abundance.

Codon Usage Analysis.

Codon counts per coding sequence were determined from the *A. fumigatus* A1163 ASM15014v1 cds fasta file available on Ensembl Fungi using R version 4.3.0 (2023-04-21) and the Biostrings Package (47). Plots and correlation analyses were produced as described in the text using R package ggplot2 version 3.4.4 (48).

tRNA gene distance calculation.

The distance between mRNA and nearest tRNA gene was determined by extracting coordinates from the *A. fumigatus* A1163 ASM15014v1.57 gff3 file (Ensembl Fungi) and comparing annotated tRNA and mRNA features using bedtools (v2.31.0) *closest* (49). mRNA elements on short contigs lacking tRNAs were removed from the downstream analyses.

Data and statistical analysis.

Statistical analyses were performed in GraphPad Prism 10 or using R version 4.3.0 (2023-04-21) in R Studio Version 2023.06.0+421 (2023.06.0+421) as described in detail in the specific methods sections or figure legends as appropriate.

RESULTS

Deletion of *mod5* confers 5-fluoroorotic acid and 5-fluorocytosine resistance.

A. fumigatus relies on rapid growth and a coordinated stress response to establish infections in the human host (50). As orthologs of Mod5 serve as regulatory hubs for stress response in bacteria, we sought to identify molecular tradeoffs upon deletion of *mod5* in a eukaryotic pathogen (21,22,51). To investigate this potential phenomenon, we sought to delete the corresponding IPTase gene in *A. fumigatus*. Using FungiDB, we identified *AFUB_093210* (hereafter called *mod5*) encoding a putative IPTase ortholog in *A. fumigatus* (52). Comparison of amino acid sequences of known Mod5-orthologs from *E. coli* (MiaA), *Homo sapiens* (TRIT1), *S. cerevisiae* (Mod5), and *S. pombe* (Tit1) revealed the conservation of all relevant domains (**Fig. S1**) (53,54). We generated a Δ*mod5* strain (**Fig. 1A, Fig. S2**), which was subjected to droplet assays to assess its growth under several stress situations (**Fig. 1**). Compared to the wild type (WT), the *mod5* knockout displayed a slightly reduced colony size on AMM plates under standard growth conditions, which was not visible on rich malt agar plates (**Fig. 1A**). We tested various stress situations that were reported to affect Δ*mod5* growth in other systems. These included the inhibition of the target of rapamycin (TOR) kinase with rapamycin (38), translational frameshifting induced by hygromycin, triggering of the amino acid starvation response with 3-amino-triazole (3-AT; (55)), interfering with the β-(1,3)-d-glucan or ergosterol biosynthesis (caspofungin, tebuconazole, itraconazole and voriconazole; (56)), and disruption of DNA and RNA stability with 5-fluoroorotic acid (5-FOA) and 5-fluorocytosin (5-FC; (57); (**Fig. 1B**)).

Treatment of Δ*mod5* with 3-AT resulted in severe growth defects visible after 48 h of incubation and even more prominent after 72 h (**Fig. 1B**). 3-AT is known to inhibit histidine biosynthesis, which decreases aminoacylation of $tRNA^{His}$ and activates the amino acid starvation responses known as cross-pathway control (CPC) and/or general amino-acid control (GAAC; (55,58-60)).

It was found that different anticodon stem-loop tRNA modification defects result in premature CPC/GAAC induction (61), hence application of 3-AT might additionally trigger this response in Δ*mod5* resulting in the observed phenotype. Hygromycin treatment also affected the growth of the Δ*mod5* knockout, likely indicating decreased frame maintenance during translation. Inhibition of TOR using two different concentrations of rapamycin (500 ng/µL and 750 ng/µL) resulted in a growth reduction of both the wild type and Δ*mod5* compared to the AMM control. Growth on agar plates containing either 5-FOA or 5-FC was severely impeded for the wild type, whereas the Δ*mod5* strain surprisingly appeared resistant to those antifungal drugs. This resistance was even more pronounced after 72 h, in contrast to other fungal systems where IPTase knockouts displayed increased susceptibility under similar stress situations (62,63). The minimal inhibitory concentration (MIC) for Δ*mod5* was established with minor modifications to the EUCAST guidelines ((64); **Tab. S1**) as 0.4 µg/µL-0.5 µg/µL for the wild type and almost 5x fold higher for Δ*mod5* at 2 µg/µL-3 µg/µL. Further droplet growth assays on caspofungin (0.5 µg/mL and 8 µg/mL) resulted in strongly reduced growth of the *mod5* knockout, whereas on tebuconazole, itraconazole, and voriconazole three independently generated clones of the deletion strain displayed varying decline in growth compared to the wild type. Although literature reported rewiring of the i^6A_{37} substrate dimethylallyl pyrophosphate (DMAPP) towards ergosterol biosynthesis upon abolishment of the tRNA modification in *S. cerevisiae* conferring azole resistance (**Fig. S3**) (37), we could not confirm this for *A. fumigatus*. This implied that the absence of Mod5 resulted not in a general resistance against specific antifungal drugs but instead affects the susceptibility against the fluorinated pyrimidine analogues, 5-FC/5-FOA. In conclusion, both the droplet plate assays and the MIC assay suggest a surprising resistance of the *mod5* knockout against the antifungal agents 5-FC and 5-FOA.

Antifungal resistance of Δ*mod5* is conferred independently of the canonical *fcyB* axis.

We next assessed the transcriptome and proteome of the knockout strain to better understand the surprising 5-FC resistance phenotype of Δ*mod5* and assess the contribution of loss of i^6A_{37} to regulation of gene expression. Previous studies found changes in the transcriptome and proteome attributable to tRNA modification defects that resulted in the induction of starvation and stress response pathways (16,38,61,65). We hypothesized that similar changes give Δ*mod5* an advantage in coping with 5-FC. For both experiments we used mycelial balls of the wild type and the knockout from liquid cultures that were grown either for 24 h non-stressed or for 16 h of normal growth followed by 8 h with 80 ng/mL 5-FC. The material obtained was split and subjected to either RNA isolation or protein isolation for poly-A enriched RNA-Seq or label-free quantification (LFQ) proteomics. Notably, since 5-FC is converted into 5-FU and incorporated into de-novo synthesized transcripts (66), we also observed an expected minor

decrease in RNA-stability for our 5-FC-treated samples. The sequencing of both strains under both conditions were used to asses expression changes under non-stressed conditions (Δ*mod5* vs WT), 5-FC-stressed and non-stressed conditions (Δ*mod5*+5-FC vs Δ*mod5*, WT+5-FC vs WT), and 5-FC treatment only (Δ*mod5*+5-FC vs WT+5-FC) (**Fig. 2A,B**; **Table S2, Fig. S4**). From the RNA-Seq, we recognized that the Δ*mod5* knockout displayed remarkable changes to the transcriptome under standard growth conditions, inducing 156 genes and supressing 44 (**Fig. 2A**; **Table S2**). Conducting a gene ontology (GO) analysis of the differentially expressed genes (DEGs) yielded an enrichment in the "cellular compartment" category for genes encoding membrane-localized transport proteins (26 induced and 11 suppressed), hinting at changes in membrane-trafficking (**Table S3**) (67). Further inspection of the altered genes revealed expression changes of different aspects of metabolically relevant genes that included secondary and carbohydrate metabolism (**Table S4,5**). These transcriptional alterations together might suggest a general mis-sensing of the nutrient level in the environment and an adaptation process of Δ*mod5* in line with reports of multiple other tRNA modification mutants (16,38,61,65). Next, we asked if any genes of the canonical 5-FC salvaging pathway were also differentially regulated in unstressed conditions. The uptake of 5-FC is mediated by the cytosine permeases FcyB and is converted stepwise to 5-fluorouracil (5-FU) by the cytosine deaminase FcyA and uracil phosphoribosyltransferase Uprt, before feeding into RNA-biosynthesis to affect transcript stability, disrupt translation, and inhibit production of thymidylate synthase to impede DNA-synthesis (66,68,69). In addition to the three canonical proteins it was recently established that two other proteins, UrkA and UrhB, are also involved in *A. fumigatus* 5-FC metabolism (69); however, no detectable changes in Δ*mod5* under non-stressed conditions were observed.

To broadly assess the response to 5-FC stress, we interrogated the stress-dependent changes observed by RNA-Seq more closely. As expected, treatment of the wild type and *mod5* knockout with 5-FC resulted in dramatic changes of both transcriptomes. The wild type displayed 3,645 DEGs (1,745 induced genes, 1,900 suppressed genes), while Δ*mod5* showed expression changes of 3,122 genes (1,586 induced genes, 1,536 suppressed genes) (**Fig. 2A**; **Table S2**) after 5-FC stress. We again checked for any significant changes of the 5-FC metabolizing pathway but only observed a slight upregulation of *urkA* ($\log_2$ fold change: 1.005) in the *mod5* knockout. Consequently, we analysed the substantial changes observed for both strains to understand which pathways might be activated to contribute to the resistance phenotype. A GO-term analysis (biological processes) revealed that both the wild type and the knockout displayed similar transcriptional changes embodied by an induction of translation-relevant genes (**Fig. 2B**; **Table S6,7**), including many ribosome biogenesis and rRNA processing genes. Similar effects upon 5-FC treatment could be observed in other pathogenic

fungi like *C. albicans* and *C. glabrata*, probably indicating a compensatory effect to cope with increased translational defects (70-72). Both strains appeared to activate DNA damage response pathways (e.g. *AFUB_009830*, *AFUB_009910*, *AFUB_026490*), but the effect only reached statistical significance in the knockout, likely due to higher variability in the wild-type results (**Fig. 2B**; **Table S6,7**). Both strains seemingly suffered from DNA damage by 5-FU and hence, in response, activated DNA safe-guarding mechanisms (66). Moreover, various GO-terms implied differential regulation of transmembrane transport proteins (e.g. "transmembrane transport", "hydrogen ion transmembrane transport") for both strains (**Fig. 2B**; **Table S6,7**). Similar changes of the transmembrane transporter regulation as well as DNA repair/recombination activity were also reported in other fungal species like *S. cerevisiae* upon 5-FC treatment (70,73,74).

These results suggest that *A. fumigatus* might adapt to the 5-FC threat by both compensating for the potential damage caused by the drug and by adjusting the transmembrane transport to limit nutrient uptake and metabolic activity—a well-documented strategy to deal with toxic stressors (75). Indeed, both strains executed a shift in carbohydrate metabolism and redox regulation ("carbohydrate metabolic process", "cellular carbohydrate metabolic process", "oxidation-reduction process"; **Fig. 2B**; **Table S6,7**), including suppression of genes relevant for energy generation (e.g., *aldA* (*AFUB_077440*), *cycA* (*AFUB_028740*), *sdh1* (*AFUB_041300*), *sdh2* (*AFUB_057960*)), production of energy reserves like glycogen or trehalose (e.g., *exg1* (*AFUB_004010*), *exg4* (*AFUB_025210*), *treA* (*AFUB_046050*)) and membrane-associated electron transport and energy conservation (e.g., *mcr1* (*AFUB_004880*), *osm1* (*AFUB_082020*)). All these transcriptional changes point to an alteration of mitochondrial energy generation and an adaptive process preventing 5-FC/5-FU induced DNA/RNA damage of the organelle. Indeed, in cancer cells, 5-FU caused a reduction of ATP production and led to mitochondria fragmentation (76), making it conceivable that similar mitochondrial damage may occur in *A. fumigatus*.

Finally, we performed a transcriptome comparison of both 5-FC-challenged wild-type and Δ*mod5* strains to further explain the observed phenotype, beyond the similarities described above. GO-term analysis intriguingly revealed that the tRNA modifier knockout strongly induces metabolically relevant genes that are involved in amino acid biosynthesis (e.g. "cellular amino acid metabolic process", "arginine biosynthetic process", "branched-chain amino acid biosynthetic process", "carboxylic acid metabolic process"; **Fig. 2B**; **Table S8**). Similar to other fungal species, the amino acid starvation response in *A. fumigatus* is controlled by the transcription factor CpcA and the cross-pathway control (CPC) system (77). This virulence-relevant pathway is canonically triggered by a decline of amino-acylated tRNAs, which in the

case of 5-FC treatment is known to increase rapidly due to the incorporation of 5-fluorouridine triphosphate (5-FUTP), a derivative of 5-FU (66). The compensation for this effect is also evident in the RNA-Seq dataset as seen in the GO-analysis of the mutant +/- 5-FC treatment ("tRNA aminoacylation for protein translation"; **Fig. 2B**) resulting in the induction of 13 aminoacyl tRNA-synthetases (aaRS), of which 10 are also upregulated in the wild type (*AFUB_008430*, *AFUB_013200*, *AFUB_019010*, *dps1* (*AFUB_019690*), *AFUB_029660*, *AFUB_052080*, *AFUB_053050*, *AFUB_053460*, *AFUB_058260*, *AFUB_087990*). Nevertheless, the induction of the CPC upon 5-FC treatment appears to be stronger in Δ*mod5* than the wild type, likely due to premature activation as previously reported (16,38,61,65).

Proteins with significantly reduced abundance in Δ*mod5* are enriched in Cysteine, Tyrosine, and Tryptophan codons.

The link between tRNA modification and translation led us to hypothesize that the proteome would display differences compared to the transcriptome in the knockout. We performed LC-MS/MS based label-free quantification on the wild-type and Δ*mod5* strains using proteins collected simultaneously from the same exact samples as in the RNA-Seq experiment. We identified 4,908 proteins common in all conditions, including both strains under non-stressed and 5-FC stressed conditions (WT: 5,551 proteins, Δ*mod5*(KO): 5,556 proteins, WT+5-FC: 5,117, Δ*mod5*(KO)+5-FC: 5,337 proteins; **Table S9-12**). Due to the stringency of the Bonferroni-Hochberg analysis and the potential of missing many other true differentially abundant proteins, we performed an analysis using the two-tailed Welch´s *t*-test (78). Using this approach, we identified many proteins differing in abundance by at least two-fold (**Fig. 3A**; **Fig.S5A-D**). In line with the transcriptome dataset, we saw comparable effects for the induced/suppressed proteins in the Δ*mod5* and wild-type strains upon non-stressed and 5-FC stressed conditions (Δ*mod5* vs WT: 69 induced, 142 suppressed; WT+5-FC vs WT: 179 induced, 387 suppressed; Δ*mod5*+5-FC vs Δ*mod5*: 201 induced, 187 suppressed; Δ*mod5*+5-FC vs WT+5-FC: 12 induced, 14 suppressed; **Fig. 3A**).

To determine whether Mod5 influenced the relationship between transcript expression and protein abundance, we plotted Z-scored protein abundances against Z-scored transcriptome data for the wild type and Δ*mod5* strains (**Fig. S5E,F**). As expected, we observed a clear correlation between the proteome and transcriptome in the wild type, but also somewhat surprisingly for the knockout, suggesting that *mod5* deletion did not overly skew translation. Both analyses resulted in moderate positive correlations as demonstrated by Pearson-correlation coefficients of (r) = 0.59 for the wild type and (r) = 0.58 for the Δ*mod5*. The plots are overlaid with selected GO-categories linked to various biological process categories by keyword to assess alterations to specific gene functions (e.g., mitochondria) as implicated in

the transcriptomics. There were no obvious differences between the different groups, suggesting that the linear relationship between the transcriptome and proteome was not disrupted by *mod5* deletion.

We next assessed individual genes more specifically by assessing potential Mod5 modification-tuneable transcripts (MoTTs) (79,80). MoTTs are transcripts whose translation is regulated by tRNA modifications. We rationalized that the deletion of *mod5* and ablation of i^6A_{37} might manifest in the proteome as Mod5-dependent MoTTs. Since the Mod5 tRNA-targets for *A. fumigatus* are not known, we assessed all codons and focused our attention on highly conserved codons from the literature (16). Pearson correlation coefficients were calculated for each codon number (number of codons per coding sequence (CDS)) and respective codon frequency (specific codon / total codons in a CDS) compared to protein abundance (**Fig. 3B, Fig. S7, S8, Tab. S13**). A negative correlation suggested a tRNA modification was required for proper translation, whereas a positive correlation suggested Mod5 activity decreased translation. We included comparisons of 5-FC treated and untreated samples to aid in finding codon-dependent deregulation (i.e. MoTTs) of specific proteins (**Fig. 3B-D, Fig. S7, S8**). Most predicted Mod5 codons exhibited small, but significant negative correlations, with serine codons being the notable exception (16). A few unexpected codons did show slight positive (e.g., arginine) or negative correlations (e.g., histidine, proline), which may warrant further investigation in the future. The tyrosine codons (and to a lesser extent cysteine and tryptophan codons) were negatively correlated with protein abundance in the knockout under normal growth conditions, but no major differences were observed during 5-FC stress, suggesting that additional mechanisms may be involved in promoting antifungal resistance to 5-FC beyond tRNA modification. We conclude that the changes observed for the proteomics closely resemble those observed for the transcriptomics and are apparently mildly attributed to traditional Mod5-dependent MoTTs as seen for the correlation with the modification of tyrosine-, cysteine-, and tryptophan-recognizing tRNA.

5-FC treatment triggers cross-pathway control in *A. fumigatus.*

The transcriptome and proteome datasets both indicated a substantial activation of genes involved in amino acid biosynthesis upon loss of *mod5* and/or 5-FC treatment (**Fig. 2B**, **Table S2**, **14-17**). Many of these signal cascades are known to be part of the evolutionarily conserved cross-pathway control (CPC) system that is regulated by the transcription factor CpcA (orthologue of Gcn4; (77)). CpcA and Gcn4 are both controlled by various translational and transcriptional regulatory layers, whereas the *cpcA* gene bears an additional auto-regulatory mechanism amplifying its own expression (81). We made use of this feature by applying quantitative reverse-transcription PCR (qRT-PCR) to measure the expression of *cpcA* and one

of its client genes *argB* under standard AMM-growth conditions of the wild-type and Δ*mod5* strains (**Fig. 4A,B**, non-shaded bars) (81). In agreement with other reports from tRNA modification mutants, the deletion of *mod5* in *A. fumigatus* resulted in a similar premature activation of the CPC by inducing the expression of *cpcA* and *argB* 1.5-fold (61). To elucidate if Δ*mod5* also altered *cpcA*/*argB* induction upon CPC-activation, we quantified expression in 3-AT treated mycelial balls, a known canonical trigger of this pathway (81). The two strains expectedly induced *cpcA* and *argB*, whereas the wild type displayed a 5.4-fold change and Δ*mod5* only a ≈4-fold change in comparison to the respective non-induced mRNA levels (**Fig. 4A**, shaded bars). When we repeated the experiment treating the wild type and tRNA modification knockout with 5-FC, we detected an induction of *cpcA* and *argB* in both strains (wild type: ≈8.5-fold and ≈2-fold, Δ*mod5*: ≈5-fold and ≈8-fold) in line with our transcriptional analysis (**Fig. 4B**, shaded bars). Surprisingly, while the induction of *cpcA* in the wild type appeared to be stronger than the one found in Δ*mod5*, the *argB* level seemed to be substantially higher in the knockout. This suggests that either CpcA activity is differentially modulated in the Δ*mod5* strain, or more compellingly, that alternative transcription factors are activated to control *argB* expression in the absence of Mod5.

Overexpression of $tRNA^{Tyr}_{G\Psi A}$ does not reverse the 5-FC resistance of Δ*mod5*.

The resistance of Δ*mod5* to the antifungal agent 5-FC is likely multifaceted, as the deletion already resulted in alterations to the transcriptome and proteome under normal growth conditions (**Fig. 2-4**). Similar changes have been reported for other tRNA modification mutants, and in each case the phenotypes were rescuable by the overexpression of the respective, majorly affected tRNA (38,39,61,65). Although Mod5 has an additional role in tRNA-mediated gene silencing, we hypothesized that resistance was attributed to the tRNA modification defect and corresponding translational impedance. We attempted to revert the 5-FC phenotype by providing an excess of the Mod5 tRNA target with the greatest negative correlation from our previous analysis and consistent with i^6A-bearing tRNAs conserved in other organisms (**Fig. S8**) (16). We chose $tRNA^{Tyr}_{G\Psi A}$, which encodes the codon UAC with the highest frequency among the downregulated proteins (**Fig. 3B-D**, **Fig. S7, S8**, **Table S13**) and also the only existing iso-decoder for tyrosine in *A. fumigatus* according to GtRNAdb (82). We created wild-type and Δ*mod5* strains containing an additional $tRNA^{Tyr}_{G\Psi A}$ gene under the control of a TetOn promoter and induced with doxycycline after confirming tRNA overexpression by northern blot to test for rescue of select phenotypes using droplet assays, (**Fig. 5, Fig. S6**).

Droplet assays on 3-AT supplemented AMM-agar plates (without doxycycline) recapitulated the Δ*mod5* phenotype, whereas the strain containing the tRNA-overexpression construct displayed a slight growth improvement (**Fig. 5**, top panel). This could be explained by the well-

known leakiness of the TetOn promoter (40). Induction of the promoter with doxycycline resulted in improved growth of Δ*mod5* on 3-AT (48 h and 72 h) in line with the proposed rescue effect by overexpression of hypomodified $tRNA^{Tyr}_{G\Psi A}$ (**Fig. 5**, +dox induction). Interestingly, the wild-type strain containing the same overexpression construct displayed similarly improved growth under normal conditions and after induction of hypomodified $tRNA^{Tyr}_{G\Psi A}$, supportive of a general role for $tRNA^{Tyr}_{G\Psi A}$ in 3-AT stress response. Similar droplet assays with either 5-FC or hygromycin resulted in varying phenotypes. Contrasting the findings with 3-AT, overexpression of $tRNA^{Tyr}_{G\Psi A}$ in Δ*mod5* did not revert the resistance phenotype of either stress. Notably, the wild type displayed a partial rescue on hygromycin upon tRNA overexpression (**Fig. 5**). These findings imply a more complicated interplay of tRNA overexpression, translation, and stress response in the Δ*mod5* strain. Since a higher than normal dose of $tRNA^{Tyr}_{G\Psi A}$ resulted only in a partial rescue of the modification deficient strain on the tested stressors it can be assumed that multiple tRNAs (e.g. cy-$tRNA^{Cys}_{GCA}$) might be functionally affected by lack of i^6A, necessitating a more challenging, combined tRNA-overexpression approach.

Deletion of mod5 results in higher expression of protein-coding genes closer to tRNA genes.

tRNA gene-mediated silencing is a conserved system among eukaryotes that supresses transcription initiation, reliant on Mod5 to bind to pre-tRNA-transcripts in close proximity to RNA polymerase II (Pol II) promoters (35). The exact distances between tRNA gene(s) and Pol II-dependent genes for sufficient tRNA gene-mediated silencing is poorly understood. Calculation of average distances between tRNA genes and protein-coding genes combined with our transcriptional dataset indeed resulted in interesting correlations (**Fig. 6, Fig. S9**). It appeared that on average the induced genes in Δ*mod5* had a much closer proximity to tRNA genes (≈54 kb) as compared to the suppressed ones (≈95 kb), although this difference was not as prominent anymore upon 5-FC treatment, likely due to the massive transcriptional changes that occur (**Fig. 2A**). This analysis provides an additional perspective on the observed transcriptional changes in the knockout implying a more prominent involvement of Mod5-dependent tRNA gene-mediated silencing in transcriptional regulation of *A. fumigatus*. Moreover, this data reveals another intriguing way to consider how the lack of a fungal IPTase, and consequent inactivation of the corresponding transcriptional regulatory axis, could lead to an induction of Mod5-regulated genes and facilitate 5-FC resistance.

DISCUSSION

Antifungal resistance poses a major threat to the human population and puts at risk our already limited repertoire of antifungal drugs. Our understanding of antifungal drug resistance

mechanisms centers primarily on genetic mutations, with limited examples of more transient forms of resistance. Here, we describe a case of accidental resistance in *A. fumigatus* driven by deletion of a tRNA modification enzyme capable of contributing to tRNA-mediated gene silencing (Mod5) that illustrates a potential molecular trade-off involved in reaching resistance. Our data support a model where the loss of the collective activities of Mod5 primes the cellular environment for enhanced resistance to the antifungal drugs 5-FC and 5-FOA at the cost of optimal gene expression.

tRNA modifying enzymes, including Mod5, have mostly been investigated in non-pathogenic fungi like *S. cerevisiae* or *S. pombe* (16), with limited consideration of antifungal drug susceptibility or resistance. *S. cerevisiae* Δ*mod5* was shown to exhibit increased susceptibility to 5-FU, the toxic derivative of the antifungal drug 5-FC, and an increased azole-resistance through formation of Mod5-amyloids and subsequent ablation of i^6A (37,62). Together with studies showing the importance of IPTases in bacterial pathogens, we hypothesized that Mod5 could serve as a hub to coordinate responses to environmental stresses, including antifungal drugs in the stress-tolerant human fungal pathogen, *A. fumigatus* (21,22).

As expected, the *A. fumigatus mod5* knockout displayed sensitivity to agents like 3-AT and hygromycin, similar to many other anticodon stem-loop-tRNA modification deficient mutants (16,83). Surprisingly, the knockout grew on agar plates supplemented with 5-FC and 5-FOA, with a roughly 5-fold higher MIC than the wild type (**Fig. 1B**, **Table S1**). 5-FC has a documented low activity on *A. fumigatus* at neutral pH, where the fungus uses PacC and the CCAAT binding complex (CBC) to suppress the expression of purine cytosine transporter *fcyB* (68). This mechanism allows the fungus to effectively stop the uptake of 5-FC and is only reversed upon acidic environmental pH. Other forms of 5-FC resistance can be caused by mutation of downstream effectors of the 5-FC salvaging system including *fcyA*, *uprt*, *urkA*, and *urhB* (66,68,69). Interestingly, by performing a transcriptome and proteome analysis of the wild type and Δ*mod5* under non-stressed and 5-FC-stressed conditions, we were unable to find any deregulation of the five 5-FC metabolizing genes. The only exception was a slight upregulation of *urkA* in the 5-FC-treated Δ*mod5* strain (**Table S2**), which encodes for a protein that converts 5-fluorouridine to 5-fluorouridine monophosphate (5-FUMP); however, deletion of *urkA* only confers slight resistance (69), suggesting that deregulation of the salvage pathway factors are not likely responsible for the Δ*mod5* phenotype.

A closer interrogation of the transcriptional reprogramming induced upon 5-FC treatment of the wild type and knockout indicated similar pronounced adaptive stress responses. This included the prevention of DNA damage and translational impedance caused by 5-FC/5-FU,

alongside a deregulation of various transmembrane transporters consistent with observations from other non-pathogenic and pathogenic fungi (**Fig.2B, Table S2,6-8**; (66,70-72)). Transcriptomics revealed an induction of amino acid starvation responsive genes in Δ*mod5*, which was also partly observed in non-stressed conditions (**Fig. 2B**, **Table S2,8**). We identified these changes as part of cross-pathway control (CPC), which is regulated by the transcription factor CpcA to regulate over 500 genes (77,81). Quantification of transcriptionally autoregulated *cpcA,* as well as one client gene *argB,* confirmed premature activation of the CPC in the knockout, similar to Δ*mod5* in *S. cerevisiae* (61); but revealed substantial differences upon 3-AT and 5-FC treatment (**Fig. 4A,B**). Both agents led to CPC activation, but surprisingly the *argB* mRNA levels were significantly higher in Δ*mod5* than in the wild type upon 5-FC stress. These results were surprising, since Δ*mod5* was highly susceptible to 3-AT unlike 5-FC, and we had hypothesized that this susceptibility was caused by additional activation of the prematurely induced CPC (61,65,83,84).

Mod5 has two major functions conserved in eukaryotes; the i^6A_{37} modification of specific tRNAs, and a role in tRNA gene-mediated silencing (16,35). Each could potentially contribute to the observed 5-FC resistance phenotype of the *mod5* deletion. The ablation of tRNA modifications in the anticodon stem-loop influences translational capacity and proteome stability resulting in the reprogramming of the transcriptome and activation of premature starvation response programs (61,65,83). In agreement, we observed an induction of starvation responses like the CPC in Δ*mod5* (**Fig. 2B**, **4A,B**), but also a shift in many pathways, e.g., in carbohydrate metabolism (**Table S7**). One explanation for this effect might be offered by MoTTs that are enriched for i^6A-dependent codons and therefore display a decreased translational efficiency in the knockout (79). In line with this hypothesis, our proteomic and codon-frequency analyses in non-stressed and 5-FC-stressed conditions displayed a negative correlation for (potential i^6A-dependent) tyrosine, cysteine, and tryptophan, and a positive correlation for arginine codons with protein abundance in the knockout (**Fig. 3B-D**, **Fig. S7, S8**). Of note, certain tRNA modifiers (*trm61* (*AFUB_069660*), *AFUB_015050* (*TYW4* in *S. cerevisiae*), *trm82* (*AFUB_005430*), and *AFUB_090820* (*QRI7* in *S. cerevisiae*)) were also among the decreased proteins in Δ*mod5*, potentially implying a more coordinated change of the epitranscriptome than initially expected (**Table S14**).

Many phenotypes observed for tRNA modification-deficient mutants can be rescued by providing an excess of the affected hypomodified tRNA(s) (26,65,85). Applying this strategy to Δ*mod5* transformed with an additional TetOn promoter-controlled $tRNA^{Tyr}_{G\Psi A}$ gene failed to completely rescue the phenotypes under different stressors (**Fig. 5**). The tRNA overexpression on 3-AT rescued the knockout growth defect and provided an advantage to the wild type, while

the phenotypes on hygromycin and 5-FC were unchanged. It is known from other tRNA modifier mutants that a combined tRNA overexpression is necessary in some cases to perform an efficient rescue (26). Since Mod5 is known to modify multiple tRNAs in yeast and we found hints of multiple modified isodecoders in *A. fumigatus* (**Fig. 3B, Fig. S8,** $tRNA^{Cys}_{GCA}$), we suspect that additional overexpression might be necessary to revert growth defects (16), although there was no significant negative correlation observed between wild type and knockout under 5-FC stress (**Fig. S8**). Notably, the strategy performed here for tRNA overexpression seemed to only result in a mild excess of $tRNA^{Tyr}_{GUA}$, which might also influence the rescue efficiency on the *mod5* knockout phenotypes (**Fig. S6**).

Finally, the involvement of Mod5 in tRNA gene-mediated silencing offers another mechanism to explain *mod5* deletion and 5-FC resistance (35). We performed a correlation analysis on tRNA gene-to-protein-coding gene distances with the transcriptome data and found an overall closer proximity of induced genes in the knockout (**Fig. 6, Fig. S9**). This correlation might hint to a scenario where the ablation of Mod5 results in inactivation of tRNA gene-mediated silencing and an induction of genes contributing to antifungal resistance against 5-FC. It is then interesting to hypothesize that the lack of Mod5-modifications and tRNA gene-mediated silencing might function similarly to epimutation-based mechanisms linked to antifungal resistance in other organisms, including fungal pathogens (86,87).

In conclusion, we provide data for an unexpected mechanism of *A. fumigatus* resistance against the antifungal drug 5-fluorocytosine, occurring after deletion of the tRNA modifier and tRNA gene-mediated silencing effector, Mod5. The molecular trade-off of losing transcriptional/translational control to boost antifungal resistance represents an interesting concept and could prove to be a more prevalent strategy in other fungal pathogens.

DATA AVAILABILITY

The mass spectrometry proteomics data were deposited in the ProteomeXchange Consortium via the PRIDE partner repository (88) with the dataset identifier PXD048351. The mRNA-Seq dataset can be found on GEO under identifier GSE251655.

SUPPLEMENTARY DATA

Supplementary Data are available at NAR online.

ACKNOWLEDGEMENTS

We would like to thank both Axel Brakhage and Amelia Barber for helpful discussions of this manuscript. We would also like to thank Bhawana Israni for excellent technical assistance.

FUNDING

The work presented here was generously supported by the Federal Ministry for Education and Research (BMBF: https://www.bmbf.de/), Germany, Project FKZ 01K12012 “RFIN – RNA-Biologie von Pilzinfektionen”. Additional funding support came from the Deutsche Forschungsgemeinschaft (DFG; German Research Foundation) under Germany´s Excellence Strategy – EXC 2051 – Project-ID 390713860, the DFG-funded Collaborative Research Center/Transregio FungiNet 124 ‘Pathogenic fungi and their human host: Networks of Interaction’ (210879364, project INF and Z2), and the BMBF-funded “PerMiCCion” project (Project ID 01KD2101D). The authors declare no conflicts of interest.

CONFLICT OF INTEREST

The authors declare no conflict of interest.

REFERENCES

1. Brown, G.D., Denning, D.W., Gow, N.A., Levitz, S.M., Netea, M.G. and White, T.C. (2012) Hidden killers: human fungal infections. *Sci Transl Med*, **4**, 165rv113.
2. Bongomin, F., Gago, S., Oladele, R.O. and Denning, D.W. (2017) Global and multi-national prevalence of fungal diseases—estimate precision. *Journal of fungi*, **3**, 57.
3. Denning, D.W. (2024) Global incidence and mortality of severe fungal disease. *The Lancet Infectious Diseases*.
4. Coordination, G., Alastruey-Izquierdo, A., Organization, W.H. and Organization, W.H. (2022). Organización Mundial de la Salud (OMS).
5. Latgé, J.-P. and Chamilos, G. (2019) *Aspergillus fumigatus* and Aspergillosis in 2019. *Clinical microbiology reviews*, **33**, 10.1128/cmr. 00140-00118.
6. Bertuzzi, M., Hayes, G.E., Icheoku, U.J., Van Rhijn, N., Denning, D.W., Osherov, N. and Bignell, E.M. (2018) Anti-Aspergillus activities of the respiratory epithelium in health and disease. *Journal of Fungi*, **4**, 8.
7. Heinekamp, T., Schmidt, H., Lapp, K., Pähtz, V., Shopova, I., Köster-Eiserfunke, N., Krüger, T., Kniemeyer, O. and Brakhage, A.A. (2015), *Seminars in immunopathology*. Springer, Vol. 37, pp. 141-152.
8. Houšť, J., Spížek, J. and Havlíček, V. (2020) Antifungal drugs. *Metabolites*, **10**, 106.
9. Wall, G. and Lopez-Ribot, J.L. (2020) Current antimycotics, new prospects, and future approaches to antifungal therapy. *Antibiotics*, **9**, 445.
10. Yao, Z.-W., Lu, X., Shen, C. and Lin, D.-F. (2014) Comparison of flucytosine and fluconazole combined with amphotericin B for the treatment of HIV-associated cryptococcal meningitis: a systematic review and meta-analysis. *European journal of clinical microbiology & infectious diseases*, **33**, 1339-1344.
11. Verweij, P.E., Lucas, J.A., Arendrup, M.C., Bowyer, P., Brinkmann, A.J., Denning, D.W., Dyer, P.S., Fisher, M.C., Geenen, P.L. and Gisi, U. (2020) The one health problem of azole resistance in *Aspergillus fumigatus*: Current insights and future research agenda. *Fungal Biology Reviews*, **34**, 202-214.
12. Rhodes, J., Abdolrasouli, A., Dunne, K., Sewell, T.R., Zhang, Y., Ballard, E., Brackin, A.P., van Rhijn, N., Chown, H. and Tsitsopoulou, A. (2022) Population genomics confirms acquisition of drug-resistant *Aspergillus fumigatus* infection by humans from the environment. *Nature microbiology*, **7**, 663-674.
13. Lorenz, C., Lünse, C.E. and Mörl, M. (2017) tRNA modifications: impact on structure and thermal adaptation. *Biomolecules*, **7**, 35.

14. Koh, C.S. and Sarin, L.P. (2018) Transfer RNA modification and infection - Implications for pathogenicity and host responses. *Biochim Biophys Acta Gene Regul Mech*, **1861**, 419-432.
15. Phizicky, E.M. and Hopper, A.K. (2010) tRNA biology charges to the front. *Genes & development*, **24**, 1832-1860.
16. Schweizer, U., Bohleber, S. and Fradejas-Villar, N. (2017) The modified base isopentenyladenosine and its derivatives in tRNA. *RNA Biol*, **14**, 1197-1208.
17. Golovko, A., Hjälm, G., Sitbon, F. and Nicander, B. (2000) Cloning of a human tRNA isopentenyl transferase. *Gene*, **258**, 85-93.
18. Dihanich, M.E., Najarian, D., Clark, R., Gillman, E.C., Martin, N.C. and Hopper, A.K. (1987) Isolation and characterization of *MOD5*, a gene required for isopentenylation of cytoplasmic and mitochondrial tRNAs of *Saccharomyces cerevisiae*. *Molecular and cellular biology*.
19. Laten, H., Gorman, J. and Bock, R.M. (1978) Isopentenyladenosine deficient tRNA from an antisuppressor mutant of *Saccharomyces cerevisiae*. *Nucleic acids research*, **5**, 4329-4342.
20. Väre, V.Y., Eruysal, E.R., Narendran, A., Sarachan, K.L. and Agris, P.F. (2017) Chemical and conformational diversity of modified nucleosides affects tRNA structure and function. *Biomolecules*, **7**, 29.
21. Durand, J., Björk, G.R., Kuwae, A., Yoshikawa, M. and Sasakawa, C. (1997) The modified nucleoside 2-methylthio-N6-isopentenyladenosine in tRNA of *Shigella flexneri* is required for expression of virulence genes. *Journal of bacteriology*, **179**, 5777-5782.
22. Fleming, B.A., Blango, M.G., Rousek, A.A., Kincannon, W.M., Tran, A., Lewis, A.J., Russell, C.W., Zhou, Q., Baird, L.M. and Barber, A.E. (2022) A tRNA modifying enzyme as a tunable regulatory nexus for bacterial stress responses and virulence. *Nucleic acids research*, **50**, 7570-7590.
23. Lee, K.-T., So, Y.-S., Yang, D.-H., Jung, K.-W., Choi, J., Lee, D.-G., Kwon, H., Jang, J., Wang, L.L. and Cha, S. (2016) Systematic functional analysis of kinases in the fungal pathogen *Cryptococcus neoformans*. *Nature communications*, **7**, 12766.
24. Choi, Y., Hyeon, H., Lee, K. and Bahn, Y.-S. (2023) Sua5 catalyzing universal t6A tRNA modification is responsible for multifaceted functions of the KEOPS complex in *Cryptococcus neoformans*. *mSphere*, e00557-00523.
25. Alings, F., Scharmann, K., Eggers Aracena, C.E., Böttcher, B., Sokołowski, M., Shvetsova, E., Sharma, P., Roth, J., Rashiti, L. and Glatt, S. (2023) Ncs2* mediates in vivo virulence of pathogenic yeast through sulphur modification of cytoplasmic transfer RNA. *Nucleic acids research*.
26. Zhang, Y., Wang, Y., Fan, J., Zhu, G. and Lu, L. (2022) *Aspergillus fumigatus* Elongator complex subunit 3 affects hyphal growth, adhesion and virulence through wobble uridine tRNA modification. *PLoS Pathog*, **18**, e1010976.
27. Li, G., Dulal, N., Gong, Z. and Wilson, R.A. (2023) Unconventional secretion of *Magnaporthe oryzae* effectors in rice cells is regulated by tRNA modification and codon usage control. *Nature Microbiology*.
28. Dabravolski, S. (2020) Multi-faceted nature of the tRNA isopentenyltransferase. *Funct Plant Biol*, **47**, 475-485.
29. Martin, N. and Hopper, A.K. (1982) Isopentenylation of both cytoplasmic and mitochondrial tRNA is affected by a single nuclear mutation. *Journal of Biological Chemistry*, **257**, 10562-10565.
30. Gillman, E.C., Slusher, L.B., Martin, N.C. and Hopper, A.K. (1991) MOD5 translation initiation sites determine N6-isopentenyladenosine modification of mitochondrial and cytoplasmic tRNA. *Molecular and cellular biology*.
31. Najarian, D., Dihanich, M.E., Martin, N.C. and Hopper, A.K. (1987) DNA sequence and transcript mapping of *MOD5*: features of the 5′ region which suggest two translational starts. *Molecular and cellular biology*, **7**, 185-191.
32. Slusher, L.B., Gillman, E.C., Martin, N.C. and Hopper, A.K. (1991) mRNA leader length and initiation codon context determine alternative AUG selection for the yeast gene *MOD5*. *Proceedings of the National Academy of Sciences*, **88**, 9789-9793.

33. Boguta, M., Hunter, L.A., Shen, W.-C., Gillman, E.C., Martin, N.C. and Hopper, A.K. (1994) Subcellular locations of MOD5 proteins: mapping of sequences sufficient for targeting to mitochondria and demonstration that mitochondrial and nuclear isoforms commingle in the cytosol. *Molecular and cellular biology*, **14**, 2298-2306.
34. Tolerico, L.H., Benko, A.L., Aris, J.P., Stanford, D.R., Martin, N.C. and Hopper, A.K. (1999) *Saccharomyces cerevisiae* Mod5p-II contains sequences antagonistic for nuclear and cytosolic locations. *Genetics*, **151**, 57-75.
35. Pratt-Hyatt, M., Pai, D.A., Haeusler, R.A., Wozniak, G.G., Good, P.D., Miller, E.L., McLeod, I.X., Yates, J.R., 3rd, Hopper, A.K. and Engelke, D.R. (2013) Mod5 protein binds to tRNA gene complexes and affects local transcriptional silencing. *Proc Natl Acad Sci U S A*, **110**, E3081-3089.
36. Read, D.F., Waller, T.J., Tse, E., Southworth, D.R., Engelke, D.R. and Smaldino, P.J. (2017) Aggregation of Mod5 is affected by tRNA binding with implications for tRNA gene-mediated silencing. *FEBS Lett*, **591**, 1601-1610.
37. Suzuki, G., Shimazu, N. and Tanaka, M. (2012) A yeast prion, Mod5, promotes acquired drug resistance and cell survival under environmental stress. *Science*, **336**, 355-359.
38. Lamichhane, T.N., Arimbasseri, A.G., Rijal, K., Iben, J.R., Wei, F.Y., Tomizawa, K. and Maraia, R.J. (2016) Lack of tRNA-i6A modification causes mitochondrial-like metabolic deficiency in *S. pombe* by limiting activity of cytosolic tRNATyr, not mito-tRNA. *Rna*, **22**, 583-596.
39. Lamichhane, T.N., Blewett, N.H., Crawford, A.K., Cherkasova, V.A., Iben, J.R., Begley, T.J., Farabaugh, P.J. and Maraia, R.J. (2013) Lack of tRNA modification isopentenyl-A37 alters mRNA decoding and causes metabolic deficiencies in fission yeast. *Molecular and cellular biology*, **33**, 2918-2929.
40. Kelani, A.A., Bruch, A., Rivieccio, F., Visser, C., Krueger, T., Weaver, D., Pan, X., Schäuble, S., Panagiotou, G. and Kniemeyer, O. (2023) Disruption of the *Aspergillus fumigatus* RNA interference machinery alters the conidial transcriptome. *RNA*, **29**, 1033-1050.
41. Weidner, G., d'Enfert, C., Koch, A., Mol, P.C. and Brakhage, A.A. (1998) Development of a homologous transformation system for the human pathogenic fungus *Aspergillus fumigatus* based on the pyrG gene encoding orotidine 5″-monophosphate decarboxylase. *Current genetics*, **33**, 378-385.
42. Pfaffl, M.W. (2001) A new mathematical model for relative quantification in real-time RT–PCR. *Nucleic acids research*, **29**, e45-e45.
43. Seelbinder, B., Wallstabe, J., Marischen, L., Weiss, E., Wurster, S., Page, L., Loffler, C., Bussemer, L., Schmitt, A.L., Wolf, T. *et al.* (2020) Triple RNA-Seq Reveals Synergy in a Human Virus-Fungus Co-infection Model. *Cell Rep*, **33**, 108389.
44. Anders, S. and Huber, W. (2010) Differential expression analysis for sequence count data. *Nature Precedings*, 1-1.
45. Southern, E. (2006) Southern blotting. *Nature protocols*, **1**, 518-525.
46. Wessel, D. and Flügge, U. (1984) A method for the quantitative recovery of protein in dilute solution in the presence of detergents and lipids. *Analytical biochemistry*, **138**, 141-143.
47. Pagès, H., Aboyoun, P., Gentleman, R. and DebRoy, S. (2023) Biostrings: Efficient manipulation of biological strings. *R package version 2.70.1*.
48. Wickham, H. and Wickham, H. (2016) *Data analysis*. Springer.
49. Quinlan, A.R. and Hall, I.M. (2010) BEDTools: a flexible suite of utilities for comparing genomic features. *Bioinformatics*, **26**, 841-842.
50. Brown, N.A. and Goldman, G.H. (2016) The contribution of *Aspergillus fumigatus* stress responses to virulence and antifungal resistance. *Journal of Microbiology*, **54**, 243-253.
51. Chanclud, E., Kisiala, A., Emery, N.R., Chalvon, V., Ducasse, A., Romiti-Michel, C., Gravot, A., Kroj, T. and Morel, J.B. (2016) Cytokinin Production by the Rice Blast Fungus Is a Pivotal Requirement for Full Virulence. *PLoS Pathog*, **12**, e1005457.
52. Basenko, E.Y., Pulman, J.A., Shanmugasundram, A., Harb, O.S., Crouch, K., Starns, D., Warrenfeltz, S., Aurrecoechea, C., Stoeckert Jr, C.J. and Kissinger, J.C. (2018)

FungiDB: an integrated bioinformatic resource for fungi and oomycetes. *Journal of Fungi*, **4**, 39.
53. Madeira, F., Pearce, M., Tivey, A.R., Basutkar, P., Lee, J., Edbali, O., Madhusoodanan, N., Kolesnikov, A. and Lopez, R. (2022) Search and sequence analysis tools services from EMBL-EBI in 2022. *Nucleic acids research*, **50**, W276-W279.
54. (2023) UniProt: the universal protein knowledgebase in 2023. *Nucleic Acids Research*, **51**, D523-D531.
55. Ahangar, M.S., Vyas, R., Nasir, N. and Biswal, B.K. (2013) Structures of native, substrate-bound and inhibited forms of *Mycobacterium tuberculosis* imidazoleglycerol-phosphate dehydratase. *Acta Crystallographica Section D: Biological Crystallography*, **69**, 2461-2467.
56. Szymański, M., Chmielewska, S., Czyżewska, U., Malinowska, M. and Tylicki, A. (2022) Echinocandins–structure, mechanism of action and use in antifungal therapy. *Journal of Enzyme Inhibition and Medicinal Chemistry*, **37**, 876-894.
57. Longley, D.B., Harkin, D.P. and Johnston, P.G. (2003) 5-fluorouracil: mechanisms of action and clinical strategies. *Nature reviews cancer*, **3**, 330-338.
58. Carsiotis, M. and Jones, R.F. (1974) Cross-pathway regulation: tryptophan-mediated control of histidine and arginine biosynthetic enzymes in *Neurospora crassa*. *Journal of Bacteriology*, **119**, 889-892.
59. Carsiotis, M., Jones, R.F. and Wesseling, A.C. (1974) Cross-pathway regulation: histidine-mediated control of histidine, tryptophan, and arginine biosynthetic enzymes in *Neurospora crassa*. *Journal of bacteriology*, **119**, 893-898.
60. Mueller, P.P. and Hinnebusch, A.G. (1986) Multiple upstream AUG codons mediate translational control of GCN4. *Cell*, **45**, 201-207.
61. Chou, H.-J., Donnard, E., Gustafsson, H.T., Garber, M. and Rando, O.J. (2017) Transcriptome-wide analysis of roles for tRNA modifications in translational regulation. *Molecular cell*, **68**, 978-992. e974.
62. Gustavsson, M. and Ronne, H. (2008) Evidence that tRNA modifying enzymes are important in vivo targets for 5-fluorouracil in yeast. *Rna*, **14**, 666-674.
63. Okamoto, M., Fujiwara, M., Hori, M., Okada, K., Yazama, F., Konishi, H., Xiao, Y., Qi, G., Shimamoto, F. and Ota, T. (2014) tRNA modifying enzymes, NSUN2 and METTL1, determine sensitivity to 5-fluorouracil in HeLa cells. *PLoS genetics*, **10**, e1004639.
64. Arendrup, M., Meletiadis, J., Mouton, J., Lagrou, K., Hamal, P. and Guinea, J. (2017) Method for the determination of broth dilution minimum inhibitory concentrations of antifungal agents for conidia forming moulds. *Def*, **9**.
65. Klassen, R., Bruch, A. and Schaffrath, R. (2020) Induction of protein aggregation and starvation response by tRNA modification defects. *Current genetics*, **66**, 1053-1057.
66. Delma, F.Z., Al-Hatmi, A.M., Brüggemann, R.J., Melchers, W.J., de Hoog, S., Verweij, P.E. and Buil, J.B. (2021) Molecular mechanisms of 5-fluorocytosine resistance in yeasts and filamentous fungi. *Journal of Fungi*, **7**, 909.
67. Priebe, S., Kreisel, C., Horn, F., Guthke, R. and Linde, J. (2015) FungiFun2: a comprehensive online resource for systematic analysis of gene lists from fungal species. *Bioinformatics*, **31**, 445-446.
68. Gsaller, F., Furukawa, T., Carr, P.D., Rash, B., Jöchl, C., Bertuzzi, M., Bignell, E.M. and Bromley, M.J. (2018) Mechanistic Basis of pH-Dependent 5-Flucytosine Resistance in *Aspergillus fumigatus*. *Antimicrob Agents Chemother*, **62**.
69. Sastre-Velasquez, L.E., Dallemulle, A., Kuhbacher, A., Baldin, C., Alcazar-Fuoli, L., Niedrig, A., Muller, C. and Gsaller, F. (2022) The fungal expel of 5-fluorocytosine derived fluoropyrimidines mitigates its antifungal activity and generates a cytotoxic environment. *PLoS Pathog*, **18**, e1011066.
70. Ribeiro, G.F., Denes, E., Heaney, H. and Childers, D.S. (2021) What 'Omics can tell us about antifungal adaptation. *FEMS Yeast Research*, **21**, foab070.
71. Liu, T.T., Lee, R.E., Barker, K.S., Lee, R.E., Wei, L., Homayouni, R. and Rogers, P.D. (2005) Genome-wide expression profiling of the response to azole, polyene, echinocandin, and pyrimidine antifungal agents in *Candida albicans*. *Antimicrobial agents and chemotherapy*, **49**, 2226-2236.

72. Pais, P., Pires, C., Costa, C., Okamoto, M., Chibana, H. and Teixeira, M.C. (2016) Membrane proteomics analysis of the *Candida glabrata* response to 5-flucytosine: unveiling the role and regulation of the drug efflux transporters CgFlr1 and CgFlr2. *Frontiers in Microbiology*, **7**, 2045.
73. Zhang, L., Zhang, Y., Zhou, Y., Zhao, Y., Zhou, Y. and Cheng, J. (2002) Expression profiling of the response of *Saccharomyces cerevisiae* to 5-fluorocytosine using a DNA microarray. *International journal of antimicrobial agents*, **20**, 444-450.
74. Agarwal, A.K., Rogers, P.D., Baerson, S.R., Jacob, M.R., Barker, K.S., Cleary, J.D., Walker, L.A., Nagle, D.G. and Clark, A.M. (2003) Genome-wide expression profiling of the response to polyene, pyrimidine, azole, and echinocandin antifungal agents in *Saccharomyces cerevisiae*. *Journal of Biological Chemistry*, **278**, 34998-35015.
75. Abad, A., Fernández-Molina, J.V., Bikandi, J., Ramírez, A., Margareto, J., Sendino, J., Hernando, F.L., Pontón, J., Garaizar, J. and Rementeria, A. (2010) What makes *Aspergillus fumigatus* a successful pathogen? Genes and molecules involved in invasive aspergillosis. *Revista iberoamericana de micologia*, **27**, 155-182.
76. Yamada, S., Yamazaki, D. and Kanda, Y. (2018) 5-Fluorouracil inhibits neural differentiation via Mfn1/2 reduction in human induced pluripotent stem cells. *The Journal of toxicological sciences*, **43**, 727-734.
77. Krappmann, S. and Braus, G.H. (2005) Nitrogen metabolism of Aspergillus and its role in pathogenicity. *Medical Mycology*, **43**, S31-S40.
78. Pascovici, D., Handler, D.C., Wu, J.X. and Haynes, P.A. (2016) Multiple testing corrections in quantitative proteomics: A useful but blunt tool. *Proteomics*, **16**, 2448-2453.
79. Dedon, P.C. and Begley, T.J. (2014) A system of RNA modifications and biased codon use controls cellular stress response at the level of translation. *Chemical research in toxicology*, **27**, 330-337.
80. Bruch, A., Laguna, T., Butter, F., Schaffrath, R. and Klassen, R. (2020) Misactivation of multiple starvation responses in yeast by loss of tRNA modifications. *Nucleic Acids Research*, **48**, 7307-7320.
81. Krappmann, S., Bignell, E.M., Reichard, U., Rogers, T., Haynes, K. and Braus, G.H. (2004) The *Aspergillus fumigatus* transcriptional activator CpcA contributes significantly to the virulence of this fungal pathogen. *Molecular microbiology*, **52**, 785-799.
82. Chan, P.P. and Lowe, T.M. (2009) GtRNAdb: a database of transfer RNA genes detected in genomic sequence. *Nucleic acids research*, **37**, D93-D97.
83. Sokołowski, M., Klassen, R., Bruch, A., Schaffrath, R. and Glatt, S. (2018) Cooperativity between different tRNA modifications and their modification pathways. *Biochimica Et Biophysica Acta (BBA)-Gene Regulatory Mechanisms*, **1861**, 409-418.
84. Amarsaikhan, N., Albrecht-Eckardt, D., Sasse, C., Braus, G.H., Ogel, Z.B. and Kniemeyer, O. (2017) Proteomic profiling of the antifungal drug response of Aspergillus fumigatus to voriconazole. *International Journal of Medical Microbiology*, **307**, 398-408.
85. Nedialkova, D.D. and Leidel, S.A. (2015) Optimization of codon translation rates via tRNA modifications maintains proteome integrity. *Cell*, **161**, 1606-1618.
86. Chang, Z., Yadav, V., Lee, S.C. and Heitman, J. (2019) Epigenetic mechanisms of drug resistance in fungi. *Fungal Genetics and Biology*, **132**, 103253.
87. Billmyre, R.B. and Heitman, J. (2017) Genetic and epigenetic engines of diversity in pathogenic microbes. *PLoS pathogens*, **13**, e1006468.
88. Perez-Riverol, Y., Bai, J., Bandla, C., García-Seisdedos, D., Hewapathirana, S., Kamatchinathan, S., Kundu, D.J., Prakash, A., Frericks-Zipper, A. and Eisenacher, M. (2022) The PRIDE database resources in 2022: a hub for mass spectrometry-based proteomics evidences. *Nucleic acids research*, **50**, D543-D552.

TABLE AND FIGURE LEGENDS

Figure 1. Deletion of *mod5* (*AFUB_093210*) in *A. fumigatus* results in increased resistance against 5-FC and 5-FOA. (A) Model displaying the i^6A_{37}-modification process depending on Mod5. The right panel shows droplet growth assays for the wild-type and Δ*mod5* strains grown on malt and AMM agar for 48 h and 72 h. (B) Strains were spotted and cultivated on AMM agar plates containing either 500 ng/mL or 750 ng/mL rapamycin, 40 µg/mL hygromycin, 0.4 µg/µL 5-FOA, 40 ng/µL 5-FC, or 0.3 mM 3-AT. Wild type and Δ*mod5* grown on AMM (without DMSO) agar plates served as controls. Documentation of the different assays was carried out after 48 h and 72 h. Data are representative images from three biological replicates.

Figure 2. Wild type and Δ*mod5* transcriptome differences are inflated upon 5-FC treatment. (A) With RNA-Seq identified significant genes ($P \leq 0.01$) with a $\log_2$ fold change of at least 1 ($\log_2$ FC≥1) are given for the indicated comparisons between strains (Δ*mod5*/wild type) and growth conditions (-/+ 5-FC). Induced genes are given in yellow and suppressed ones in blue. (B) GO-terms for up- (yellow) and down-regulated (blue) genes among the different comparisons are listed according to their Bonferroni adjusted *P*-values ($-\log_{10}$) together with the respective gene numbers (grey).

Figure 3. Proteome changes mirror transcriptional alterations elucidated for the wild type and Δ*mod5* under non-stressed and 5-FC stressed conditions. (A) LC-MS/MS-identified proteins with a $\log_2$ fold change of at least 2 ($\log_2$ FC≥2) and ($P \leq 0.05$) are given for the indicated comparisons between strains (Δ*mod5*/wild type) and growth conditions (-/+ 5-FC). Proteins with increased abundance are given in yellow and decreased in blue. (B) Spearman's rank correlation coefficients were determined for the number and frequency of putative Mod5-modified codons and select codon combinations (see Table S13) in coding sequences compared to the Log_2FC values for the indicated comparisons determined in the proteomics analysis (Table S14-17). Blue and red imply a positive or negative correlation. (C,D) Plots display relative protein abundances (cut-off given in A) of the different comparisons conducted for Δ*mod5* and wild type upon different conditions (+/- 5-FC) versus Mod5-dependent codon-usage per open-reading frame (Table S13-17). Orange dots indicate samples with $P \leq 0.05$ and Log_2FC >|1|in the corresponding proteomics comparison. To be included in (B-D), a protein had to be identified in at least 2 biological replicates of one of the tested conditions.

Figure 4. Treatment with 5-FC and 3-AT induce *cpcA* expression but results in differential induction of downstream client gene *argB*. Wild-type and Δ*mod5* mycelial balls were harvested after 24 h cultivation in AMM media and subjected to RNA isolation, cDNA synthesis and qPCR to quantify *cpcA* and *argB* mRNA level. Additionally, mycelial balls of the respective strains

were treated either with 3-AT (**A**) or 5-FC (**B**) and quantified for the indicated genes. The quantifications of *cpcA*/*argB* were normalized to the *cox5* level (42). The calculated P-values are as follows: 0.05-0.01 (a-c; a'-c'; b-d); <0.01 (a-b; a'-b'; c-d; c'-d'; b'-d'). Statistical significance was calculated using a two-way ANOVA test on $\log_{10}$ transformed data. Pairwise comparisons were carried out using the Holm Sidak method. Small letters indicate statistical significance with the apostrophe (') sign differentiating between the genes (*cpcA*, *argB*). The P-value ≤ 0.05 was considered as significant.

Figure 5. $tRNA^{Tyr}_{G\Psi A}$ overexpression reverts the 3-AT but not 5-FC and hygromycin phenotype of Δ*mod5*. The droplet growth assays for the wild-type and Δ*mod5* strain, as well as the respective $tRNA^{Tyr}_{G\Psi A}$ overexpression strains, were grown for 48 h and 72 h. The strains were spotted and cultivated on AMM agar plates containing either 0.3 mM 3-AT, 40 µg/mL hygromycin, or 0.8 µg/µL 5-FC. Data are representative images from 3 biological replicates.

Figure 6. Genes induced in Δ*mod5* display a closer proximity to tRNA genes than down-regulated ones. Transcriptional data of non-stressed (clear boxes) and 5-FC stressed (checked boxes) samples were correlated with the average distances between tRNA genes and protein-coding genes. Significance was determined by Brown-Forsythe and Welch ANOVA test with Dunnett's T3 multiple comparisons test as posttest. *P*-value ***=0.0004.

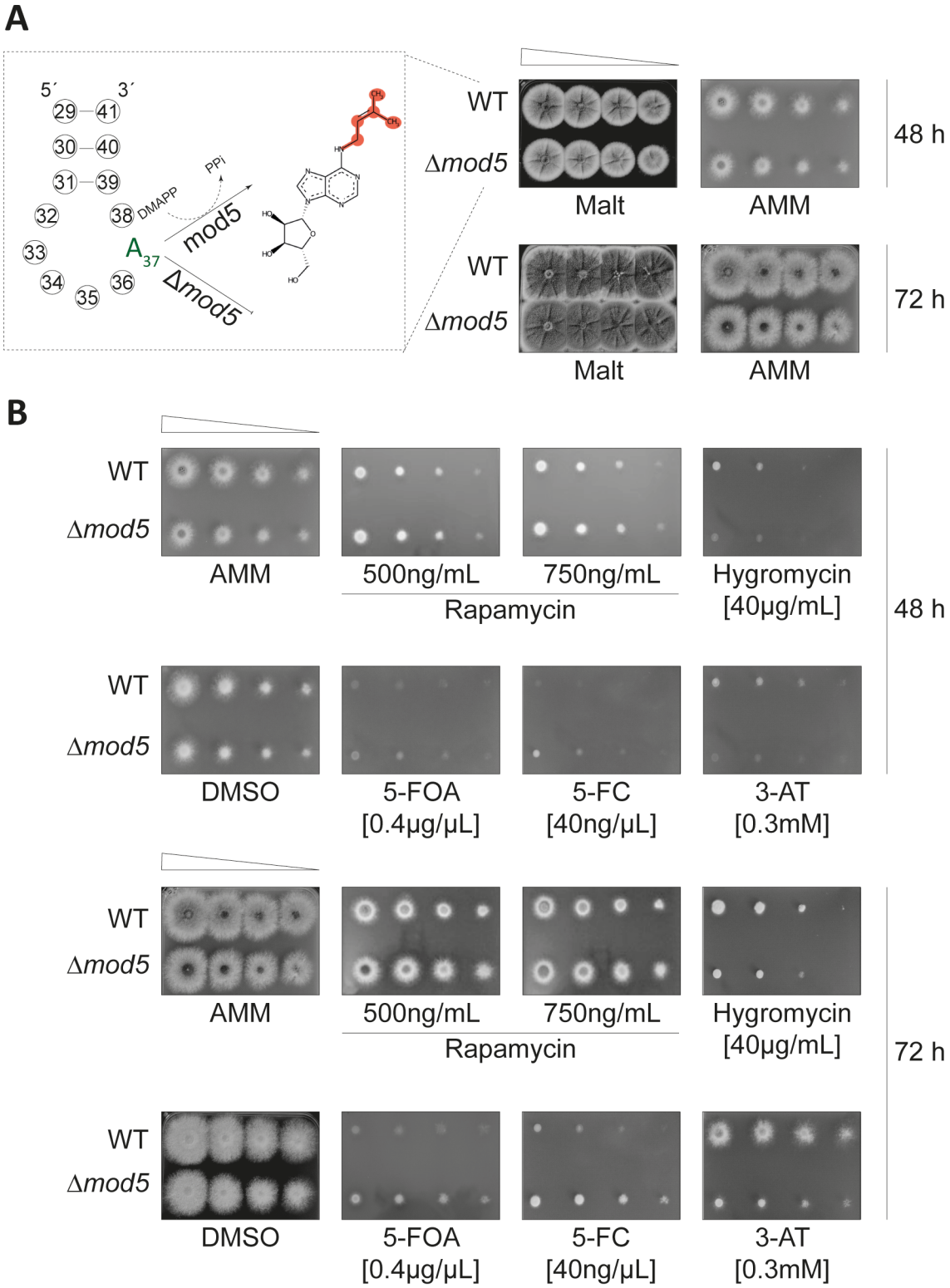
A
5´
3´
29
41
30
40
31
39
32
38
33
34
35
36
DMAPP
PPi
mod5
A37
Δmod5
WT
Δmod5
Malt
AMM
48 h
WT
Δmod5
Malt
AMM
72 h
B
WT
Δmod5
AMM
500ng/mL
750ng/mL
Rapamycin
Hygromycin
[40µg/mL]
48 h
WT
Δmod5
DMSO
5-FOA
[0.4µg/µL]
5-FC
[40ng/µL]
3-AT
[0.3mM]
WT
Δmod5
AMM
500ng/mL
750ng/mL
Rapamycin
Hygromycin
[40µg/mL]
72 h
WT
Δmod5
DMSO
5-FOA
[0.4µg/µL]
5-FC
[40ng/µL]
3-AT
[0.3mM]

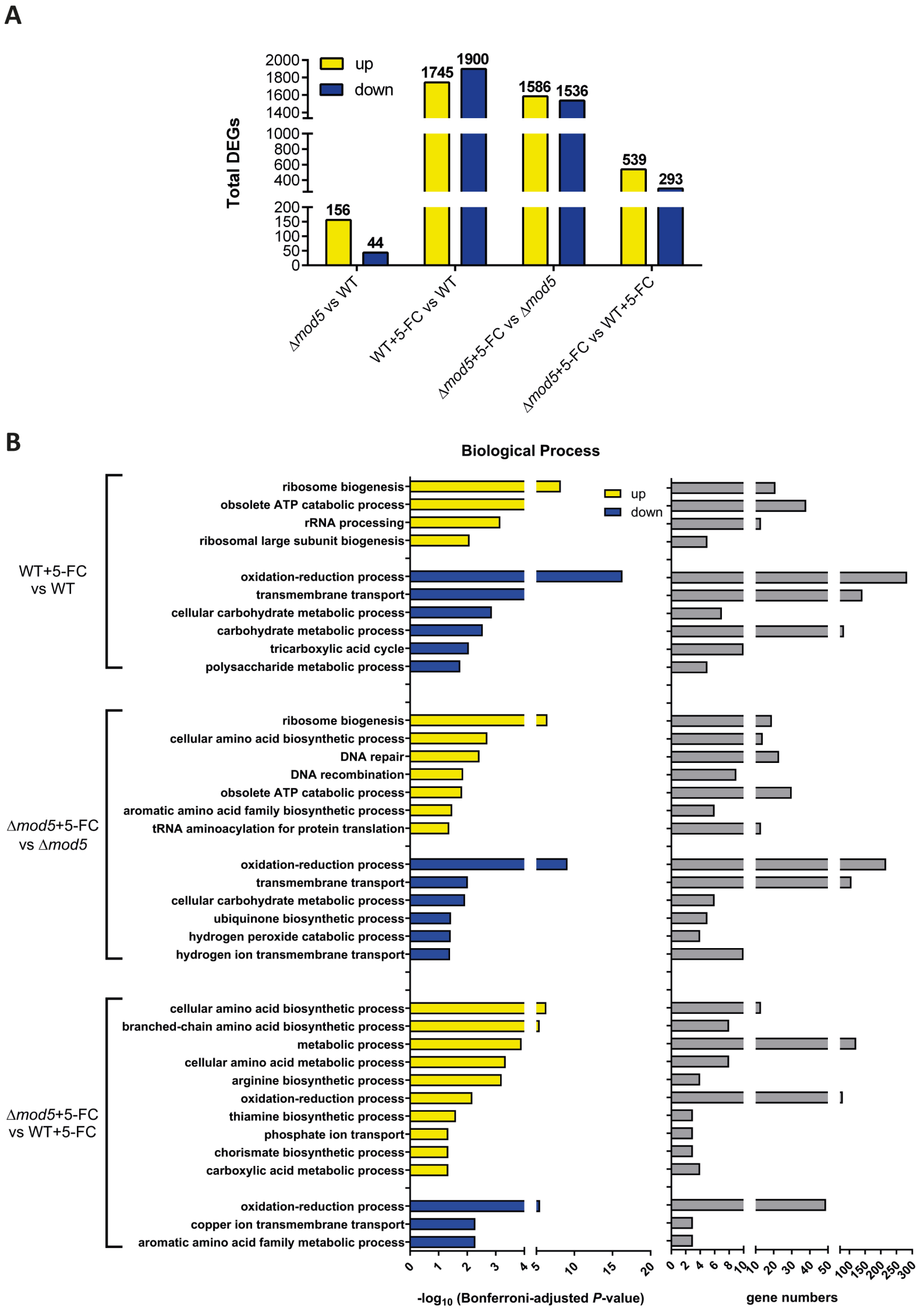
A
Total DEGs
up
down
156
44
1745
1900
1586
1536
539
293
Δmod5 vs WT
WT+5-FC vs WT
Δmod5+5-FC vs Δmod5
Δmod5+5-FC vs WT+5-FC
B
Biological Process
WT+5-FC vs WT
ribosome biogenesis
obsolete ATP catabolic process
rRNA processing
ribosomal large subunit biogenesis
oxidation-reduction process
transmembrane transport
cellular carbohydrate metabolic process
carbohydrate metabolic process
tricarboxylic acid cycle
polysaccharide metabolic process
Δmod5+5-FC vs Δmod5
ribosome biogenesis
cellular amino acid biosynthetic process
DNA repair
DNA recombination
obsolete ATP catabolic process
aromatic amino acid family biosynthetic process
tRNA aminoacylation for protein translation
oxidation-reduction process
transmembrane transport
cellular carbohydrate metabolic process
ubiquinone biosynthetic process
hydrogen peroxide catabolic process
hydrogen ion transmembrane transport
Δmod5+5-FC vs WT+5-FC
cellular amino acid biosynthetic process
branched-chain amino acid biosynthetic process
metabolic process
cellular amino acid metabolic process
arginine biosynthetic process
oxidation-reduction process
thiamine biosynthetic process
phosphate ion transport
chorismate biosynthetic process
carboxylic acid metabolic process
oxidation-reduction process
copper ion transmembrane transport
aromatic amino acid family metabolic process
up
down
-log10 (Bonferroni-adjusted P-value)
gene numbers

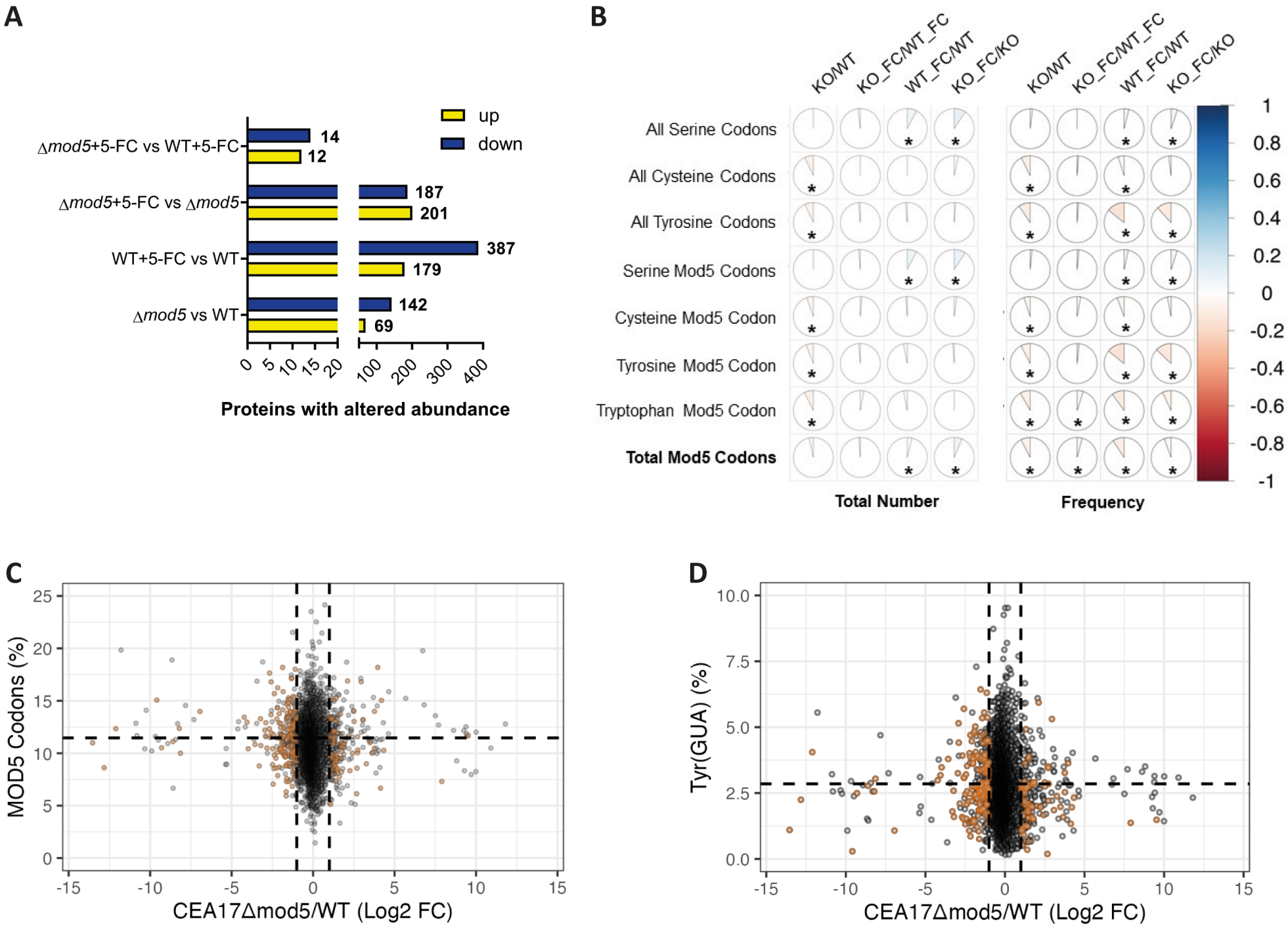
A
up
down
Δmod5+5-FC vs WT+5-FC
14
12
Δmod5+5-FC vs Δmod5
187
201
WT+5-FC vs WT
387
179
Δmod5 vs WT
142
69
0 5 10 15 20
100 200 300 400
Proteins with altered abundance
B
KO/WT
KO_FC/WT_FC
WT_FC/WT
KO_FC/KO
All Serine Codons
All Cysteine Codons
All Tyrosine Codons
Serine Mod5 Codons
Cysteine Mod5 Codon
Tyrosine Mod5 Codon
Tryptophan Mod5 Codon
Total Mod5 Codons
Total Number
Frequency
1 0.8 0.6 0.4 0.2 0 -0.2 -0.4 -0.6 -0.8 -1
C
MOD5 Codons (%)
CEA17Δmod5/WT (Log2 FC)
D
Tyr(GUA) (%)
CEA17Δmod5/WT (Log2 FC)

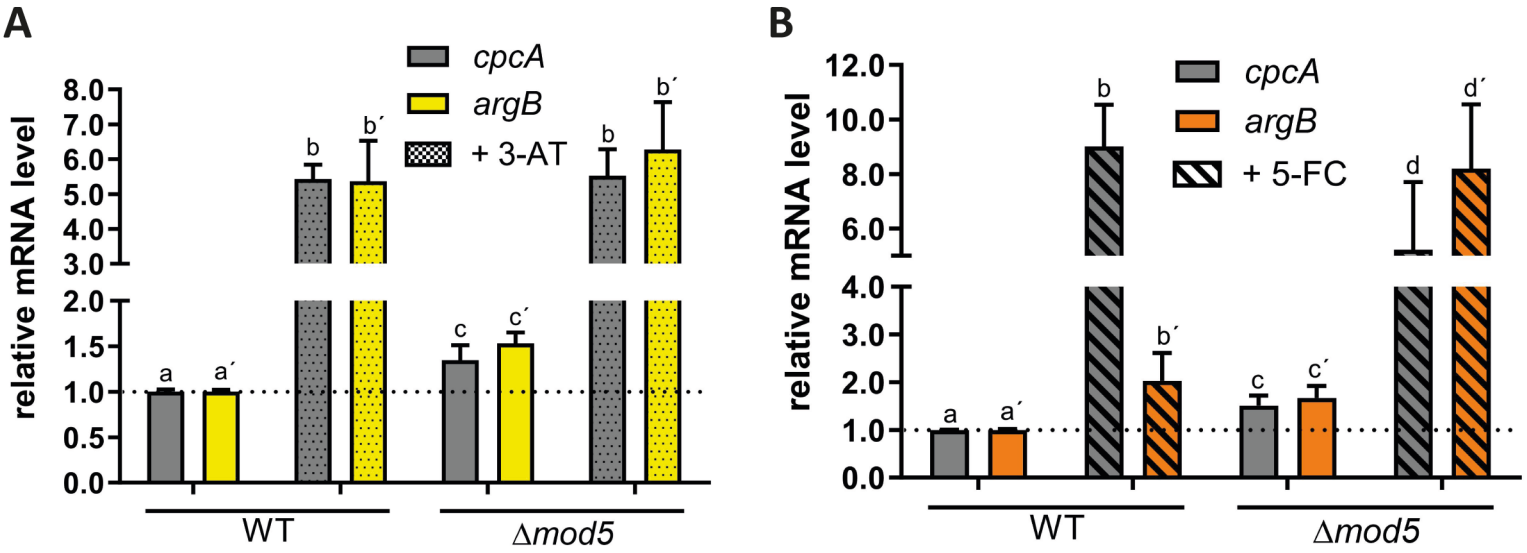
A
cpcA
argB
+ 3-AT
relative mRNA level
8.0
7.0
6.0
5.0
4.0
3.0
2.0
1.5
1.0
0.5
0.0
a
a´
b
b´
c
c´
b
b´
WT
Δmod5
B
cpcA
argB
+ 5-FC
relative mRNA level
12.0
10.0
8.0
6.0
4.0
3.0
2.0
1.0
0.0
a
a´
b
b´
c
c´
d
d´
WT
Δmod5

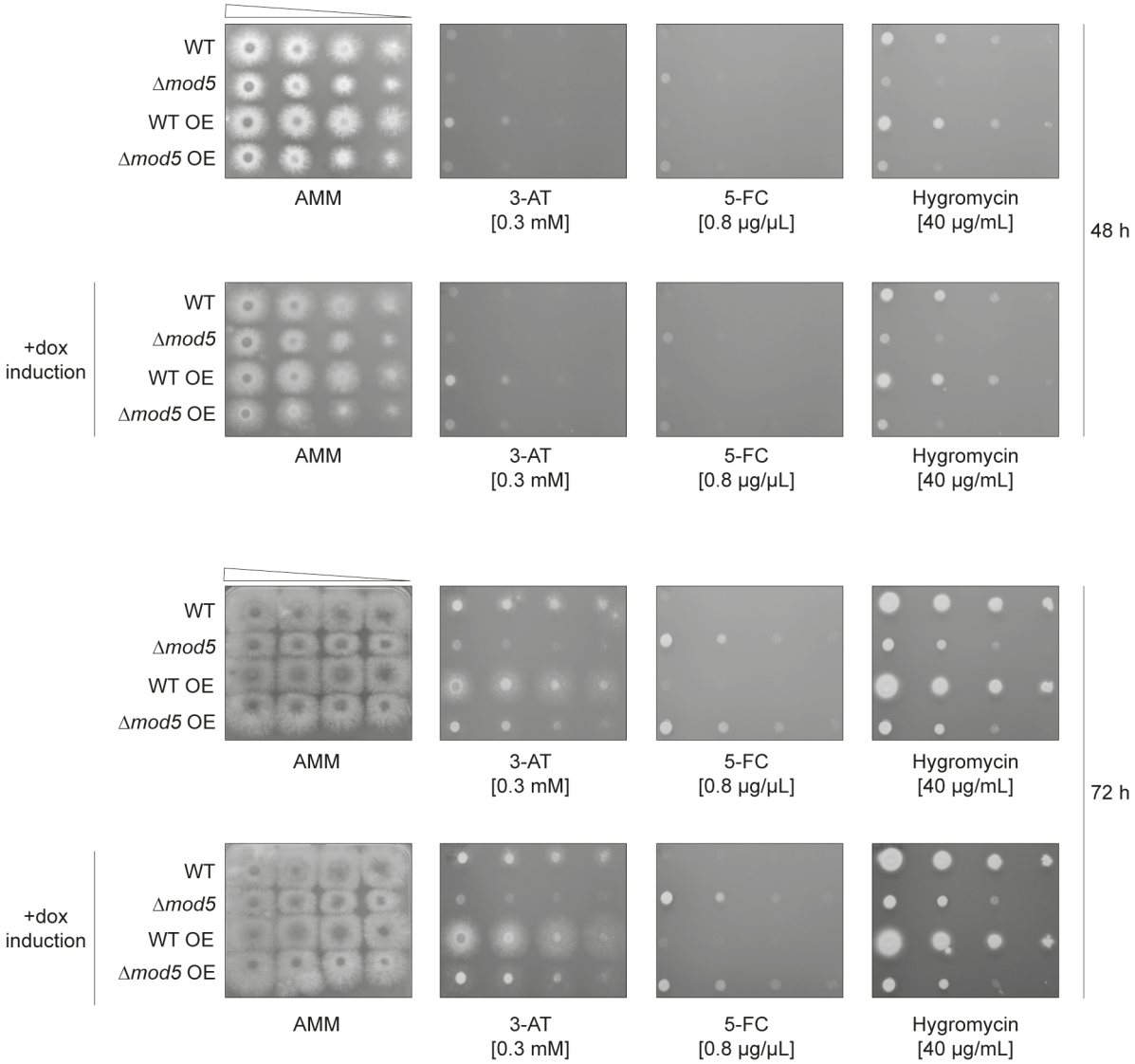
WT
Δmod5
WT OE
Δmod5 OE
AMM
3-AT
[0.3 mM]
5-FC
[0.8 µg/µL]
Hygromycin
[40 µg/mL]
48 h
+dox
induction
WT
Δmod5
WT OE
Δmod5 OE
AMM
3-AT
[0.3 mM]
5-FC
[0.8 µg/µL]
Hygromycin
[40 µg/mL]
WT
Δmod5
WT OE
Δmod5 OE
AMM
3-AT
[0.3 mM]
5-FC
[0.8 µg/µL]
Hygromycin
[40 µg/mL]
72 h
+dox
induction
WT
Δmod5
WT OE
Δmod5 OE
AMM
3-AT
[0.3 mM]
5-FC
[0.8 µg/µL]
Hygromycin
[40 µg/mL]

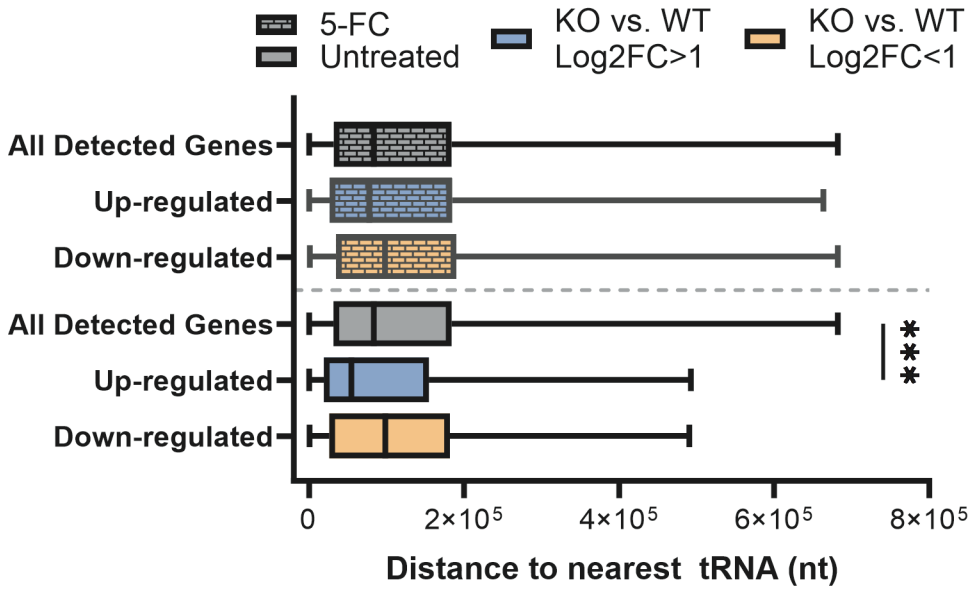
5-FC
Untreated
KO vs. WT
Log2FC>1
KO vs. WT
Log2FC<1
All Detected Genes
Up-regulated
Down-regulated
All Detected Genes
Up-regulated
Down-regulated
***
0
2×10^5
4×10^5
6×10^5
8×10^5
Distance to nearest tRNA (nt)